Infiltrative Renal Malignancies: Imaging Features, Prognostic Implications, and Mimics

David E. Sweet, MD
Ryan D. Ward, MD
Yanbo Wang, MD
Hajime Tanaka, MD
Steven C. Campbell, MD, PhD
Erick M. Remer, MD

Abbreviations: IgG4-RKD = immunoglobulin G4–related kidney disease, RCC = renal cell carcinoma, SCC = squamous cell carcinoma, UCC = urothelial cell carcinoma

RadioGraphics 2021; 41:487–508

https://doi.org/10.1148/rg.2021200123

Content Codes: CT GU OI

From the Imaging Institute (D.E.S., R.D.W., E.M.R.) and Glickman Urological and Kidney Institute (Y.W., H.T., S.C.C., E.M.R.), Cleveland Clinic, 9500 Euclid Ave, L10, Cleveland, OH 44195; Department of Urology, First Hospital of Jilin University, Changchun, China (Y.W.); and Department of Urology, Tokyo Medical and Dental University, Tokyo, Japan (H.T.). Recipient of a Certificate of Merit award for an education exhibit at the 2019 RSNA Annual Meeting. Received May 12, 2020; revision requested June 26 and received July 24; accepted August 7. For this journal-based SA-CME activity, the authors, editor, and reviewers have disclosed no relevant relationships. **Address correspondence to** D.E.S. (e-mail: *sweetd@ccf.org*).

SA-CME LEARNING OBJECTIVES

After completing this journal-based SA-CME activity, participants will be able to:

- Describe the imaging features of infiltrative renal masses depicted on cross-sectional images.
- Identify key benign and malignant renal lesions that may have an infiltrative pattern at imaging.
- Discuss the importance of recognizing the infiltrative pattern of renal masses in terms of prognosis and treatment.

See rsna.org/learning-center-rg.

Infiltrative renal malignancies are a subset of renal masses that are morphologically characterized by a poorly defined interface with the renal parenchyma. Infiltrative renal malignancies are less common but more aggressive than more typical renal malignancies and carry an overall worse prognosis. Although an infiltrative renal process often represents a malignant neoplasm, infiltrative masses include a wide spectrum of diseases including primary renal cortical, medullary, and pelvic tumors; lymphoproliferative processes; metastases; and various infectious, inflammatory, immune-mediated, and vascular mimics. The imaging features of these masses are often nonspecific, but with the appropriate history, laboratory results, and clinical context, the radiologist can help narrow the diagnosis and guide further treatment.

An invited commentary by Lee is available online.
Online supplemental material is available for this article.

Introduction

Renal masses can be characterized as expansile or infiltrative according to their morphologic growth pattern. Expansile masses have spherical growth that displaces normal parenchyma, often causing exophytic bulging of the renal contour (Figs 1, 2). The expansile pattern of growth manifests as a well-defined circumscribed mass with margins that can be delineated from the adjacent normal renal parenchyma. A pseudocapsule can result as the growing mass compresses the surrounding tissue, leading to a peripheral wall of ischemia and necrosis around the mass (1). The majority of renal masses, 94% in one series (2), demonstrate this elliptical or spherical well-encapsulated pattern due to expansile growth.

Much less commonly, renal masses exhibit infiltrative growth that involves the underlying renal architecture, with spread via interstitial proliferation of cells around nephrons, collecting ducts, and blood vessels (3). Infiltrative renal masses have a poorly defined interface with normal parenchyma and an irregular shape (nonspherical or nonelliptical) (Figs 1, 3). The infiltrative growth leads to expansion of the renal contour, with distinct preservation of the reniform shape. A mass growing by means of infiltration frequently encases the collecting system and replaces the renal sinus fat. It is important to note that occasionally, infiltrative growth can involve only a portion of the mass and may even occur as a focal ill-defined tumor margin of what would otherwise be identified as an expansile mass (4,5).

Infiltrative growth of renal neoplasms has been identified as a unique feature of clinically aggressive tumor behavior that is an independent predictor of patient survival (4–6). Infiltrative renal neoplasms are typically large at presentation, with advanced local-regional spread and early metastases. Unlike the more frequently encountered expansile renal cell carcinomas (RCCs) that are increasingly detected

TEACHING POINTS

- Radiologic identification of infiltrative features is a strong differentiator of renal tumor biology and outcomes, and these features should be routinely documented when present.
- Because of their high overall frequency, RCCs with atypical growth patterns are one of the more frequent causes of infiltrative tumors and should be considered in the differential diagnosis of an infiltrative renal mass. In particular, the presence of an infiltrative renal mass with concomitant intravascular tumor extension is highly suggestive of an atypical RCC.
- The unique combination of clinical and imaging features (infiltrative right renal mass, African American race, sickle cell trait, metastatic disease at presentation) should suggest the diagnosis of renal medullary carcinoma.
- An infiltrative renal pelvic UCC should be considered when a central, poorly marginated mass extending into the adjacent parenchyma is seen at imaging, especially if an additional lesion is identified in the urinary tract.
- The combination of infiltrative renal masses in the presence of bulky perinephric disease, widespread lymphadenopathy, splenomegaly, and bilateral involvement is suggestive of lymphoma. In many cases, patients have an established diagnosis of lymphoma at the time of imaging.

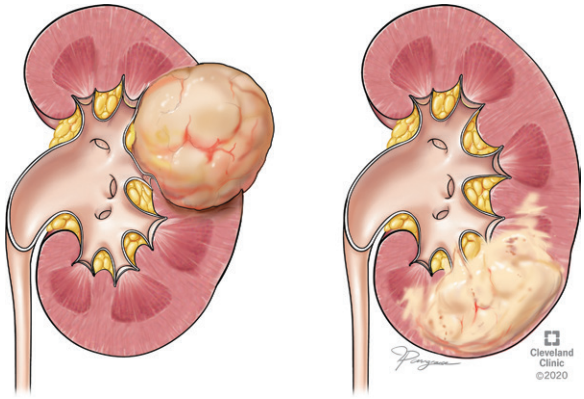

Figure 1. Expansile and infiltrative renal masses. Expansile growth (left) manifests as a well-defined spherical mass that displaces the normal parenchyma and collecting system and causes focal bulging of the renal contour. In contrast, a renal mass with infiltrative growth (right) invades the normal structures using the underlying nephrons, collecting ducts, and blood vessels as a framework for tumor growth, resulting in a poorly defined interface between the mass and the normal parenchyma and preservation of the reniform shape.

incidentally and are amenable to nephron-sparing interventions, infiltrative tumors demonstrate rapid growth leading to symptomatic manifestations (abdominal pain, palpable flank mass, and gross hematuria) and poor clinical outcomes (4,5).

Although an infiltrative renal process at imaging often represents a malignant neoplasm, interstitial cellular infiltration is nonspecific and may occur as a result of other inflammatory, autoimmune, vascular, and traumatic processes (Table 1). The infiltrative appearance is not specific to any single entity, but when this feature is considered in the context of other radiologic findings, patient history, and laboratory findings, it may help narrow the differential diagnosis and facilitate clinical management.

This review describes common and uncommon infiltrative renal masses through multimodality case examples. The clinical outcomes associated with infiltrative renal tumors are discussed to establish the prognostic value of identifying infiltration as a tumor feature. Emphasis is placed on identifying the unique clinical and imaging characteristics of each entity so that radiologists are better able to accurately diagnose these conditions.

Imaging Techniques

The initial imaging modality chosen is often based on a patient's presenting symptoms, the acuity of the symptoms, and laboratory findings. For example, in the United States, a patient presenting with hematuria will typically undergo CT urography, whereas a patient with flank pain may undergo noncontrast CT and a patient with acute kidney injury may undergo renal US, depending on the clinical setting, the subspecialty of the ordering provider, and other factors.

Conventional gray-scale and Doppler US have limited sensitivity for the detection and characterization of renal masses but are helpful in differentiating cysts from solid masses. The American College of Radiology (ACR) Appropriateness Criteria (7) do not recommend US as the initial imaging examination when a urinary tract mass is suspected in a patient who presents with hematuria (with exceptions made for pregnant and pediatric patients). In practice, many renal parenchymal masses are initially detected at US because of the rapid bedside availability of this modality in the emergency department setting, its lack of ionizing radiation, and the presence of patient contraindications to contrast-enhanced CT (eg, renal insufficiency, contrast material allergies) (8). Suspicious renal masses identified at US require additional imaging for characterization.

The US features of infiltrative renal masses include indistinctly marginated abnormal parenchymal echogenicity (either hyperechoic or hypoechoic) with enlargement and preservation of the kidney's reniform shape. While contrast-enhanced US is currently used off label in the United States, it has been shown to have high sensitivity (100%) and specificity (95%) in the characterization of an indeterminate renal mass as benign or malignant (9). The most recent ACR Appropriateness Criteria (10) added contrast-enhanced US as an appropriate initial imaging examination for an indeterminate renal mass, especially for patients in whom iodinated CT contrast material or gadolinium-based MRI contrast material is contraindicated.

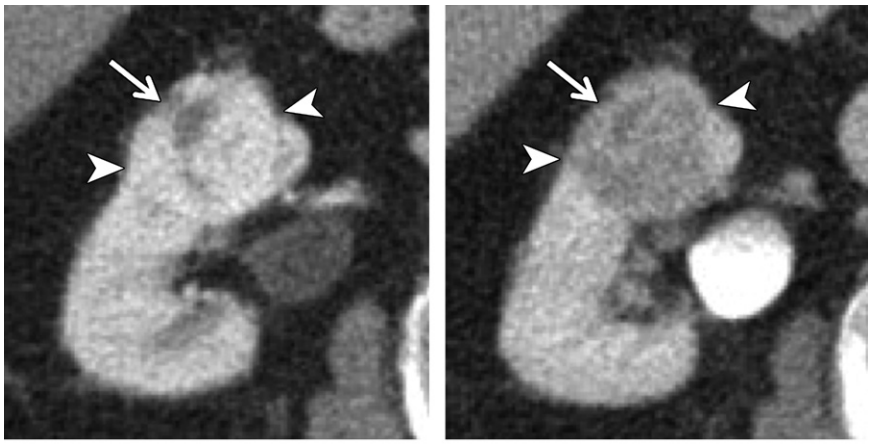

a. b.

Figure 2. Imaging features of an expansile renal mass. Axial contrast-enhanced CT images show a spherical well-marginated mass with avid enhancement during the arterial phase (arrow in **a**) and enhancement less than the renal parenchyma during the excretory phase (arrow in **b**). Exophytic bulging (arrowheads) beyond the expected normal renal contour is seen.

Table 1: Renal Malignancies with Infiltrative Growth Patterns

Renal cortical tumors
Atypical growth pattern of clear cell, papillary, and chromophobe RCCs, with or without sarcomatoid differentiation and with or without rhabdoid differentiation
Renal medullary tumors
Medullary carcinoma
Collecting duct carcinoma
Renal pelvis tumors
UCC
SCC
Metastases
Bronchogenic carcinoma
Other (eg, colorectal, gastric, and breast carcinomas)
Lymphoproliferative disease
Renal lymphoma
Renal leukemia
Renal plasmacytoma
Mimickers of renal malignancy
Acute pyelonephritis
Xanthogranulomatous pyelonephritis
Renal infarct
IgG4–RKD

Note.—IgG4-RKD = immunoglobulin G4–related kidney disease, SCC = squamous cell carcinoma, UCC = urothelial cell carcinoma.

CT or MRI with and without intravenous contrast material is essential for the evaluation of indeterminate renal masses, and especially infiltrative masses, as the presence of enhancement is central to diagnosing a potential neoplasm and defining its boundaries (10). Thin-section three-phase CT (noncontrast and contrast-enhanced corticomedullary and nephrographic phases) is the most common imaging modality for the workup of an indeterminate renal mass.

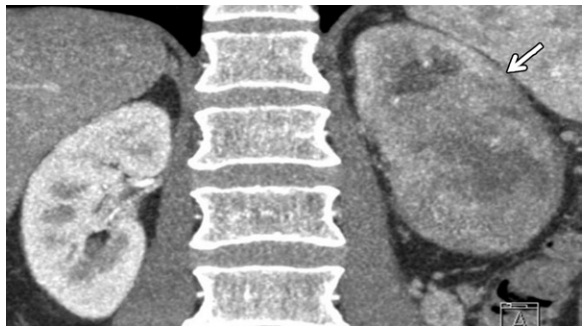

Figure 3. Imaging features of an infiltrative renal mass. Coronal contrast-enhanced CT image shows a poorly defined left renal mass enlarging the left kidney, with preservation of the reniform shape (arrow).

Contrast-enhanced MRI provides sensitivity and specificity values similar to those seen with CT for evaluating indeterminate renal masses (11,12). Contrast-enhanced CT and MRI show infiltrative masses as poorly marginated areas of diminished enhancement as compared to normal renal parenchyma. Characteristic features of infiltrative masses such as extension into the renal sinus fat and preservation of the reniform shape can also be assessed with CT and MRI. Care must be taken to evaluate for locally advanced features (ie, involvement of the renal vein, adrenal gland, or regional lymph nodes) and to evaluate the remaining abdominal viscera for disease, as infiltrative renal masses often have early distant metastases or can represent metastatic disease from a different primary tumor.

It should be noted that infiltrative renal masses confined to the parenchyma are difficult to detect at noncontrast CT, as the reniform shape is preserved and the mass-parenchyma interface is often poorly visualized because the mass and normal parenchyma have similar attenuation. If both CT and MRI contrast agents are contraindicated and contrast-enhanced US is unavailable, MRI without contrast material is preferable to CT, as

some indeterminate renal masses can be characterized using noncontrast T1-, T2-, and diffusion-weighted images (10).

Infiltrative Renal Malignancies: Clinical Outcomes

The ability to recognize infiltrative tumor growth at radiologic and histopathologic examinations has important prognostic implications. In 2011, Fukatsu et al (13) showed that the presence of an infiltrative growth pattern on histopathologic specimens of clear cell RCC is an independent risk factor for decreased disease-free survival and cancer-specific survival. In 2019, Tanaka et al (5) reviewed the imaging studies of 522 patients with locally advanced and/or aggressive histologically diagnosed renal tumors managed with partial or radical nephrectomy and found that 25% of these tumors exhibited infiltrative features at preoperative contrast-enhanced CT or MRI. Even within this high-risk population, infiltrative imaging features were found to be independent predictors of cancer-specific mortality, which was four to five times higher than the cancer-specific mortality in patients with noninfiltrative masses (Fig 4). An important point is that even a focal area of infiltration (Fig 5) on imaging studies (manifesting as a poorly defined interface with normal parenchyma) confers a significantly worse cancer-specific mortality rate, albeit not as severe as that conferred by extensive infiltration.

Similarly, in 2019, Wang et al (4) conducted a retrospective review of 280 radiographically identified renal masses with infiltrative features and found that at the time of diagnosis, the masses were typically symptomatic (68% of cases), locally advanced (stage cT3–T4, 66% of cases), and disseminated (68% of cases). Oncologic outcomes were poor, with a median time to cancer-related death of less than 5 months. These studies confirm that infiltrative renal neoplasms represent a clinically aggressive subset of disease with more adverse oncologic outcomes. As such, the preoperative identification of radiologic features of infiltrative growth can suggest the presence of clinically aggressive tumors and guide surgeons away from attempted partial nephrectomy.

Despite the prognostic value of describing infiltrative features, recent data show that radiologists at both academic and community hospitals do not routinely mention this characteristic. In a multi-institutional review of reported radiologic details regarding potentially malignant renal masses, Hu et al (14) found that only 10% of reports distinguished circumscribed or infiltrative features. In 2018, the Society for Abdominal Radiology Disease-Focused Panel on Renal Cell Carcinoma (15) concluded that describing

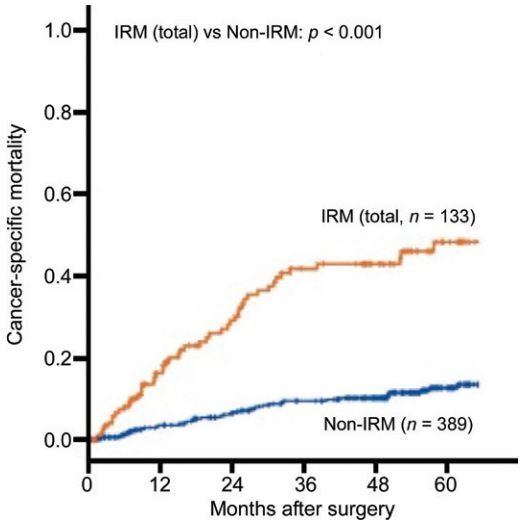

Figure 4. Graph illustrates the prognostic implications of infiltrative renal tumor features. Plot of cancer-specific mortality versus time after kidney surgery shows significantly increased mortality for radiologically identified infiltrative renal masses *(IRM)* compared with noninfiltrative masses. (Reprinted, with permission, from reference 4.)

circumscribed versus infiltrative mass margins is an essential radiologic reporting characteristic for any indeterminate renal mass. Thus, radiologic identification of infiltrative features is a strong differentiator of renal tumor biology and outcomes, and these features should be routinely documented when present.

RCC with Atypical Growth Pattern

RCC represents a group of adenocarcinomas that arise from the epithelium of the renal tubules and account for more than 85% of all renal cancers (1,16,17). Once considered to be a single histologic entity, RCC has evolved to represent a catch-all term describing a heterogeneous group of renal epithelial tumors that continues to expand as novel morphologic types are recognized with advances in genomic profiling. The characterization of RCC is still evolving, and the 2016 edition of the World Health Organization classification catalogs 14 different histologic subtypes. The clear cell (75%), papillary (10%), and chromophobe (5%) subtypes account for the majority of RCCs, while the remaining 10% consist of relatively uncommon and unclassified carcinomas (16,18).

Most conventional RCC subtypes (ie, clear cell, papillary, and chromophobe) demonstrate an expansile growth pattern, appearing as focal well-circumscribed masses, with only a small percentage manifesting as atypical infiltrative masses (Figs 6, 7). In addition to the atypical infiltrative growth of conventional RCCs, infiltrative growth often manifests in any RCC subtype with sarcomatoid or rhabdoid features (Figs 8, 9). In the

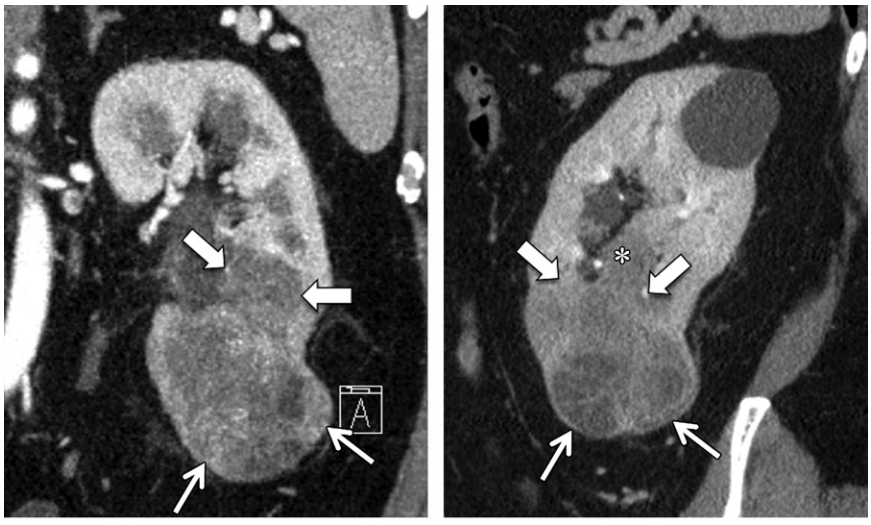

a. b.

Figure 5. Imaging features of a focally infiltrative renal mass. Coronal **(a)** and sagittal **(b)** contrast-enhanced CT images show a partially exophytic left lower pole enhancing mass (thin arrows) that is predominantly spherical and circumscribed but has an infiltrative poorly defined superior margin that is difficult to distinguish from the adjacent normal renal parenchyma (thick arrows). Focal infiltration extends into the renal sinus (* in **b**). Histopathologic analysis revealed clear cell RCC with rhabdoid differentiation.

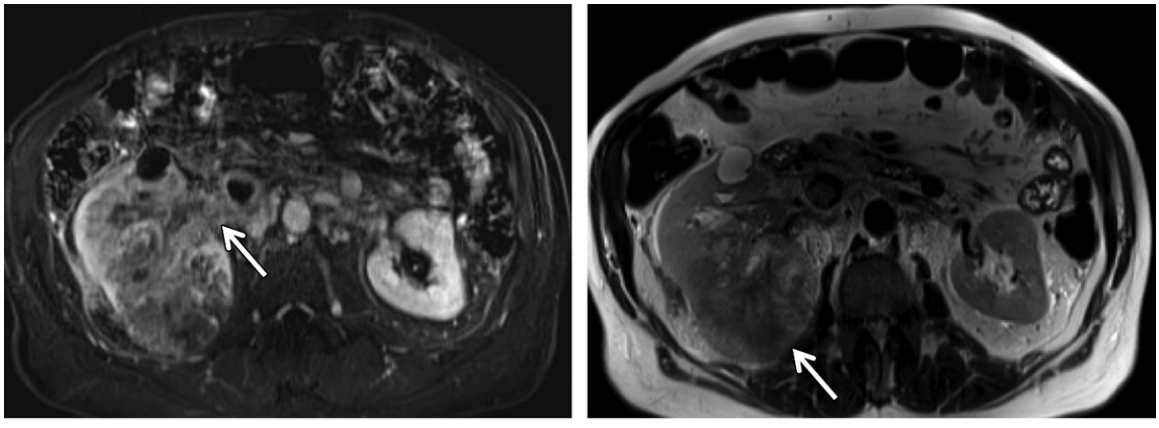

a. b.

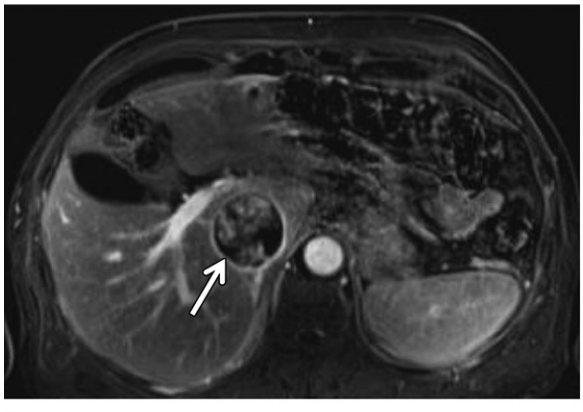

c.

Figure 6. Atypical RCC, clear cell subtype. **(a)** Axial contrast-enhanced T1-weighted fat-suppressed MR image shows an expanded right kidney with a heterogeneous poorly defined tumor infiltrating the renal parenchyma, with extension into the renal sinus and renal vein (arrow). **(b)** Axial T2-weighted MR image shows heterogeneous low signal intensity (arrow) in the mass compared to normal parenchyma. **(c)** Axial contrast-enhanced T1-weighted fat-suppressed MR image shows a dilated intrahepatic inferior vena cava containing enhancing tumor (arrow).

current World Health Organization classification of RCC, sarcomatoid or rhabdoid phenotypes are not categorized as distinct histologic entities; rather, these phenotypes reflect unique patterns of dedifferentiation that can occur in any conventional subtype. When present, these histologic features confer a much more aggressive growth pattern and an overall worse prognosis. The median survival times after diagnosis are 6–19 months for patients who have RCC with sarcomatoid features and 8 months for those who have RCC with rhabdoid features (19,20). The ability to distinguish sarcomatoid features in an RCC preoperatively has important clinical significance, as observation, ablative therapy, and nephron-sparing surgery are not recommended. The choice of systemic therapy also differs when sarcomatoid features are present (21). Sarcomatoid differentiation occurs in approximately 5%–8% of clear cell carcinomas, 2%–9% of chromophobe carcinomas, and 2%–5% of papillary carcinomas (16). Rhabdoid features occur in 3%–7% of RCC cases and are most frequently associated with clear cell carcinoma (16). Overall, approximately

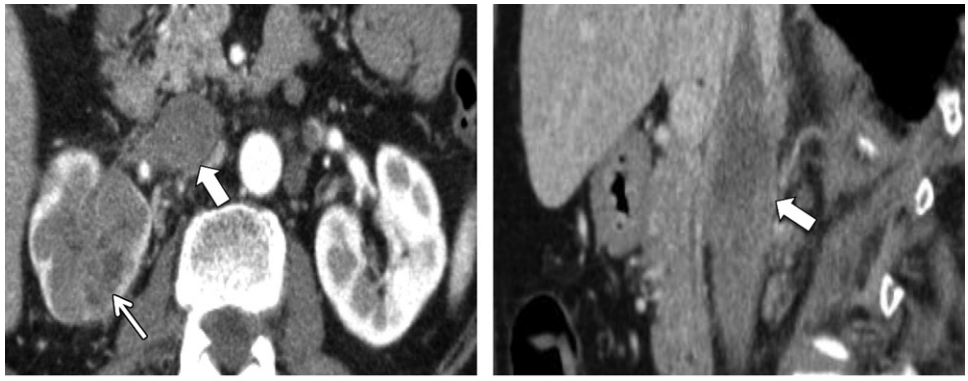

a. b.

Figure 7. Atypical RCC, papillary subtype. Axial **(a)** and sagittal **(b)** contrast-enhanced CT images show a right infiltrative renal mass (thin arrow in **a**) extending through the renal vein into the subdiaphragmatic inferior vena cava (thick arrow).

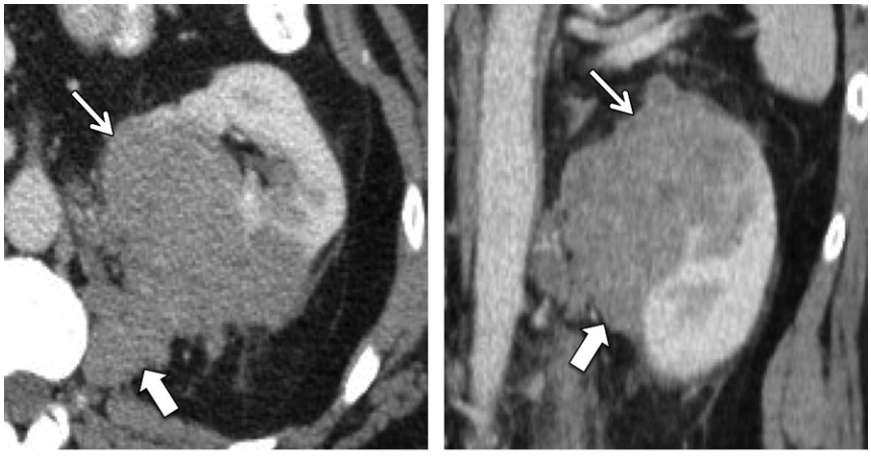

a. b.

Figure 8. RCC with sarcomatoid features. Axial **(a)** and coronal **(b)** contrast-enhanced CT images show an infiltrative left renal mass (thin arrow), with expansion through the cortex into the adjacent perinephric fat (thick arrow).

6% of RCCs demonstrate atypical or dedifferentiated infiltrative growth (2).

The US appearance of atypical RCC in the absence of contrast material is variable; therefore, US should be followed by CT or MRI if an underlying mass is suspected. Compared with conventional RCCs, which often have a round encapsulated appearance with smooth margins and variable enhancement, atypical RCCs can have an infiltrative morphology of growth with an irregular shape and a poor interface with the normal parenchyma. The infiltrative pattern may involve the entire mass or a single area within an otherwise well-circumscribed mass. The infiltrative growth often preserves the renal contour, which can be difficult to detect at noncontrast CT. At contrast-enhanced CT or MRI, the infiltrative tumor may be hyperenhancing or hypoenhancing relative to the adjacent parenchyma, and restricted diffusion may be seen.

RCCs that develop sarcomatoid or rhabdoid differentiation are often larger and more likely to have extrarenal extension with irregular margins and distant metastasis at the time of diagnosis. When present, a disrupted pseudocapsule with an invasive margin, peritumoral neovascularity, and larger peritumoral vessel size are more commonly associated with RCCs that have sarcomatoid features (22,23). Because of their high overall frequency, RCCs with atypical growth patterns are one of the more frequent causes of infiltrative tumors and should be considered in the differential diagnosis of an infiltrative renal mass. In particular, the presence of an infiltrative renal mass with concomitant intravascular tumor extension is highly suggestive of an atypical RCC.

Renal Medullary Tumors

Renal Medullary Carcinoma

Renal medullary carcinoma is a rare and aggressive tumor that arises from the renal papilla or calyceal epithelium of the renal medulla. It accounts for only 1%–2% of RCCs and is found almost exclusively in individuals with the sickle cell trait. The pathogenesis is hypothesized to be chronic hypoxia related to the hemoglobinopathy, which leads to a proliferation of the terminal

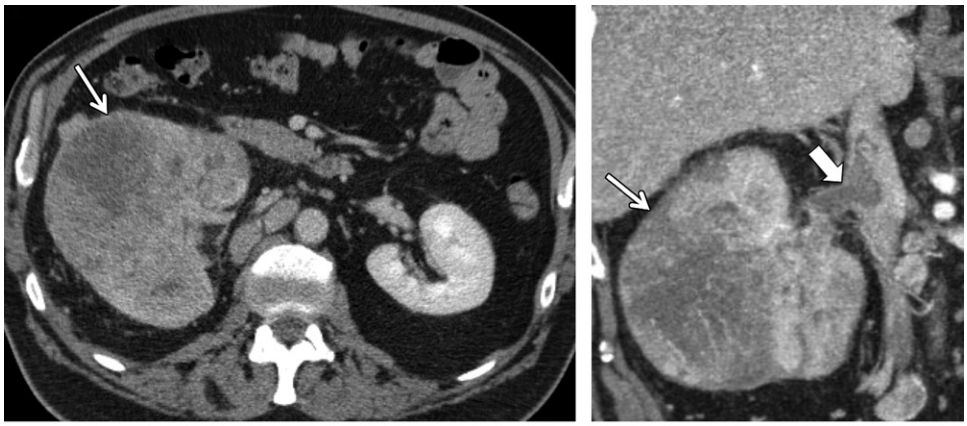

a. b.

Figure 9. RCC, clear cell subtype with sarcomatoid differentiation. Axial **(a)** and coronal **(b)** contrast-enhanced CT images show a large infiltrative mass (thin arrow) expanding the right kidney, with extension into the renal vein and inferior vena cava (thick arrow in **b**).

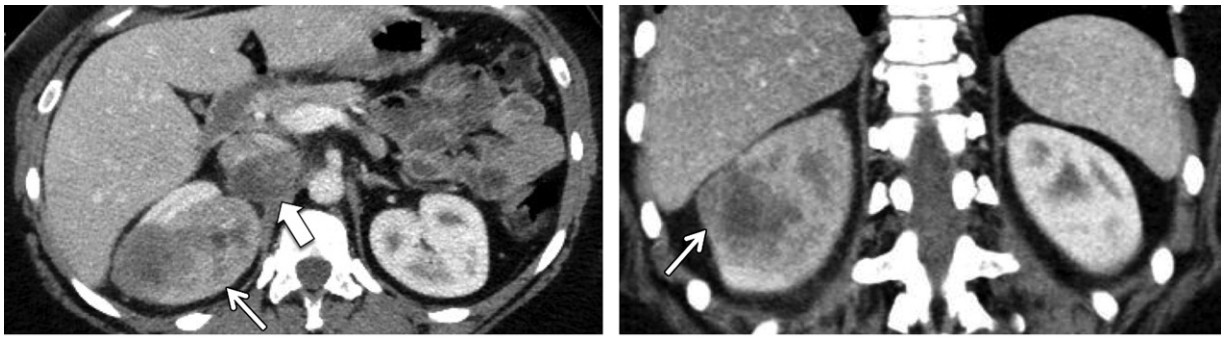

a. b.

Figure 10. Renal medullary carcinoma in a 39-year-old African American woman with sickle cell trait and right flank pain. Axial **(a)** and coronal **(b)** contrast-enhanced CT images show an infiltrative right renal mass involving the medulla, with obliteration of the sinus fat and cortical extension (thin arrow). Retrocaval lymph node metastasis (thick arrow in **a**) also can be seen.

collecting ducts and papillary epithelium that triggers a neoplastic transformation (24). Interestingly, there is no association between renal medullary carcinoma and sickle cell disease.

A systematic review of all reported cases of renal medullary carcinoma through 2013 (47 articles, 165 cases) confirmed the presence of multiple characteristic features: Sixty-seven percent of affected patients presented with hematuria and pain, 71% were male, 93% were African American, and 98% had sickle cell trait (25). The median age of affected patients was 21 years. The right kidney is preferentially affected in more than 75% of cases (26). Renal medullary carcinoma is almost never seen in patients without sickle cell trait, such that a tumor with similar morphology and immunophenotype in an individual without a hemoglobinopathy should be classified histopathologically as RCC unclassified with medullary phenotype rather than as renal medullary carcinoma (27). Renal medullary carcinoma is one of the most aggressive renal malignancies, with dismal clinical outcomes and a median survival of 13–17 months (25,28,29). The average tumor size at presentation is 6 cm, and most patients have metastatic disease at the time of presentation, most frequently involving the regional lymph nodes, lungs, liver, adrenal glands, or contralateral kidney (25).

At imaging, renal medullary carcinoma appears as a large ill-defined, poorly circumscribed tumor that is predominantly centered in the renal medulla, with extension into the renal sinus (Fig 10). Most tumors exhibit growth into the renal cortex, with perinephric and peripelvic soft tissue at the time of diagnosis. The medullary origin can be difficult to appreciate in cases of large masses. The tumor causes expansion of the affected kidney while maintaining its reniform shape. Hemorrhage and geographic necrosis are typically present, giving the tumor a heterogeneous appearance on CT images and sometimes producing a signal void on T2-weighted MR images due to susceptibility artifact related to the blood products (30,31). The unique combination of clinical and imaging features (infiltrative right renal mass, African American race, sickle cell trait,

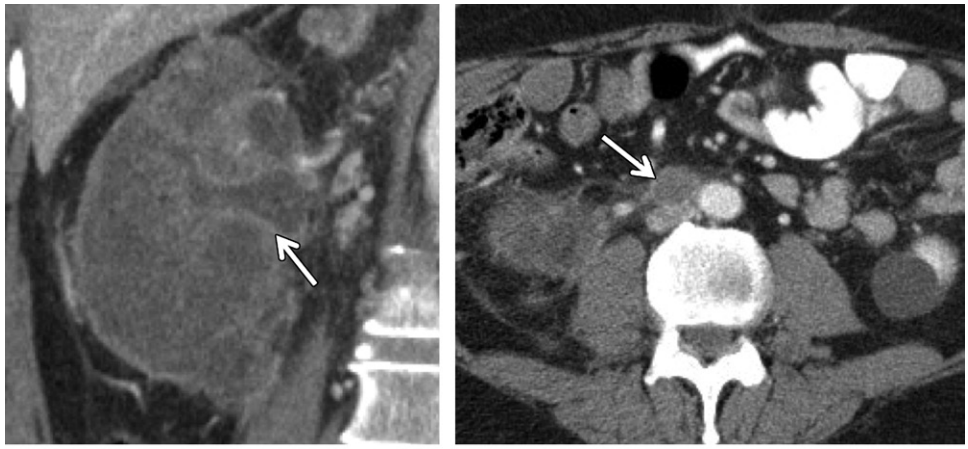

a. b.

Figure 11. Collecting duct carcinoma in a 59-year-old man with right flank pain and hematuria. **(a)** Coronal contrast-enhanced CT image shows an infiltrative right renal mass with involvement of the pelvis–proximal ureter (arrow) and areas of heterogeneous low attenuation, reflecting necrosis. **(b)** Axial CT image from the same examination shows a retroperitoneal node metastasis (arrow). Figure E1 shows an additional lung metastasis in this patient.

metastatic disease at presentation) should suggest the diagnosis of renal medullary carcinoma.

Collecting Duct Carcinoma

Collecting duct carcinoma, previously referred to as Bellini duct carcinoma, is an extremely rare aggressive renal neoplasm that arises from the distal segment of the collecting ducts of Bellini in the medullary pyramids due to epithelial dysplasia. Collecting duct carcinoma shares many histologic features with renal medullary carcinoma, and its recognition as a distinct entity is considered somewhat controversial.

Collecting duct carcinoma is considered one of the most aggressive renal tumors, with a fatal clinical course. Approximately 35%–40% of patients have distant metastases at presentation, with an average survival of 11.5 months (range, 7–17 months) (32,33). The most common sites of metastatic disease are the regional lymph nodes, lungs, and adrenal glands (34). Unlike the more common RCCs that are increasingly detected incidentally, the rapid growth of this carcinoma leads to a symptomatic presentation, with patients reporting abdominal pain, a palpable flank mass, and gross hematuria. Systemic features of anorexia, weight loss, fatigue, and fever may also occur (35).

The typical imaging appearance is that of an infiltrative mass centered in the renal medulla, with extension into the renal cortex and pelvis, along with replacement of the renal sinus fat (Fig 11). The tumor commonly has areas of necrosis and can appear multicystic related to dilated tubular structures. As the tumor is often large at presentation, with infiltration throughout the kidney and renal sinus, it can be difficult to ascertain its medullary origin. In addition, although collecting duct carcinoma primarily demonstrates infiltrative growth with the reniform shape preserved, an expansile component can occur as the tumor enlarges and extends beyond the renal capsule (23,36).

Renal Pelvic Tumors

Primary tumors of the renal pelvis and collecting system account for up to 10%–15% of neoplasms of the upper urinary tract (37–39). Renal pelvic tumors develop from the mucosal surface epithelium (referred to as urothelium) that lines the renal collecting tubules, calyces, and pelvis. UCCs account for the vast majority of renal pelvic tumors in the United States, with SCCs and mucinous adenocarcinomas representing a small number of cases. UCCs and SCCs can exhibit infiltrative growth, especially in high-grade cases, manifesting as a poorly marginated mass centered in the renal pelvis.

Urothelial Cell Carcinoma

UCC represents 90% of all renal pelvic epithelial tumors. The synonymous term *transitional cell carcinoma* is used to refer to the same entity but was replaced with UCC in the 2016 World Health Organization classification of urinary system tumors (40). Although UCCs can arise anywhere along the urothelial tract, most of them (90%) occur in the bladder, with fewer occurring in the kidney (8%) and ureter or urethra (2%). UCC has a strong predilection for spread along the ipsilateral or contralateral urinary tract; approximately 30% of patients have multifocal disease at presentation (41). The pathogenesis is thought to be due to intraluminal seeding and implantation, acquired

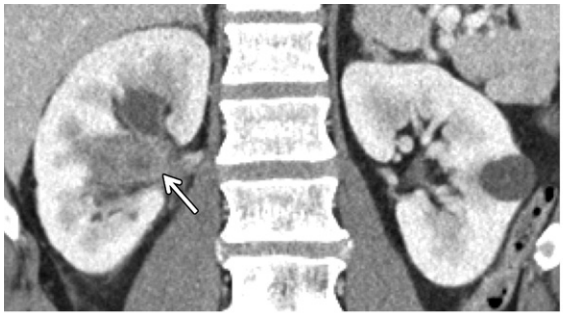

a.

b.

Figure 12. Renal pelvic UCC in a 61-year-old man with painless hematuria. Coronal **(a)** and axial **(b)** contrast-enhanced CT images show a low-attenuation infiltrative mass centered in the right pelvis (arrow in **a**) that obliterates the sinus fat and extends into the medulla (arrow in **b**).

genetic carcinogenic alterations of the urothelium from lengthy exposure to an injurious environment (referred to as field cancerization), or both. Synchronous UCC is reported to occur in 1%–2% of renal pelvic tumor cases, 2%–9% of ureteral tumor cases, and 2% of bladder tumor cases. Likewise, metachronous tumors develop within 2 years after surgical treatment in up to 50% of upper-tract UCC cases and 6% of bladder UCC cases (37). When UCCs recur, they are often higher-grade tumors and occur at a different site.

Upper-tract (kidney and ureter) UCC predominantly affects older adults between the ages of 60 and 70 years, with men affected two to four times more often than women (37,42). Cigarette smoking is a major risk factor, with exposure to other carcinogenic agents in the urine identified as another causative factor (38).

Most UCCs are small slow-growing tumors that follow a relatively benign course. However, approximately 15% of UCCs exhibit infiltrative growth; these tumors tend to behave aggressively and be more advanced at diagnosis. Infiltrative upper-tract UCCs are characterized by pelvicaliceal or ureteral irregularity related to thickening and induration of the renal pelvis and/or ureteral wall, with obliteration of at least a part of the collecting system (Figs 12, 13). The calyces can become dilated and focally obstructed from tumor invasion (oncocalyx). When the renal pelvis is involved, there is usually poorly marginated extension into the renal parenchyma that preserves the renal contour (37). Invasion of the retroperitoneum, regional lymphadenopathy, distant metastases to the lung and bones, and rarely venous tumor extension may be identified.

Contrast-enhanced CT and MRI show subtle tumor enhancement less than that of surrounding renal parenchyma. The nephrographic phase is ideal for identifying UCC parenchymal invasion, manifesting tumor involvement as a focal delay in the nephrogram. Excretory phase images demonstrate dilated calyces that may be unopacified because of tumor invasion. Large infiltrative UCCs can develop regions of necrosis, contributing to a more heterogeneous tumor appearance on CT and MR images (43). As UCC is often multifocal at manifestation, the entire urinary tract should be scrutinized for synchronous tumors if a single lesion is found (Fig 14). Likewise, there should be high suspicion for development of a metachronous lesion anywhere along the urinary tract at surveillance imaging (Fig 15). An infiltrative renal pelvic UCC should be considered when a central, poorly marginated mass extending into the adjacent parenchyma is seen at imaging, especially if an additional lesion is identified in the urinary tract.

Squamous Cell Carcinoma

SCC is the second most common malignancy of the renal pelvic urothelium after UCC, but this type of carcinoma is relatively rare, constituting 8%–15% of renal pelvic tumors and less than 1% of all renal malignancies (42,44,45). There is an increased prevalence of SCC among patients with renal calculi and in countries where the parasitic infection schistosomiasis is endemic, as chronic urothelial infection and irritation lead to squamous metaplasia. Most patients are aged 50–60 years at diagnosis and present with an insidious onset of hematuria and flank pain. Fever and additional constitutional symptoms such as anorexia, weight loss, and fatigue may also be present (42). Renal pelvic SCC is a highly aggressive tumor that primarily exhibits an infiltrative pattern of growth. SCC is usually advanced at the time of diagnosis, with a tendency to metastasize early to lung, liver, and bone (46). Consequently, the prognosis is dismal, with two-thirds of patients dying at 1 year and an overall 5-year survival rate of 13.3% (42,45).

The imaging appearance of renal pelvic SCC is that of an extensive infiltrative mass with extension into the sinus fat and parenchyma. SCC has an increased propensity for extraluminal invasion beyond the involved renal pelvis, parenchyma, and ureter. In particular, secondary extension into the psoas muscle is frequently described (42,45). Associated renal calculi are reported in 47%–58% of cases of renal pelvic SCC (45). Marked hydronephrosis due to obstruction at the

Figure 13. Poorly differentiated renal pelvic UCC in a 67-year-old woman with hematuria, leukocytosis, and left flank pain. **(a, b)** Axial **(a)** and coronal **(b)** noncontrast CT images show retroperitoneal lymphadenopathy (arrow in **a**) and an infiltrative left renal tumor that is discernible only because of its deformation of the inferior lower pole renal contour (arrow in **b**). **(c, d)** Subsequent axial **(c)** and coronal **(d)** contrast-enhanced T1-weighted MR images show a heterogeneously enhancing infiltrative left lower pole mass (thin arrow) extending into the perirenal space (thick arrow in **c**). **(e)** Coronal T2-weighted MR image shows the mass with a hypointense signal (arrow) compared with the normal parenchyma. **(f, g)** Axial diffusion-weighted MR image **(f)** and corresponding apparent diffusion coefficient map **(g)** show restricted diffusion in the areas of the left renal tumor (thin arrow) and retroperitoneal lymphadenopathy (thick arrow).

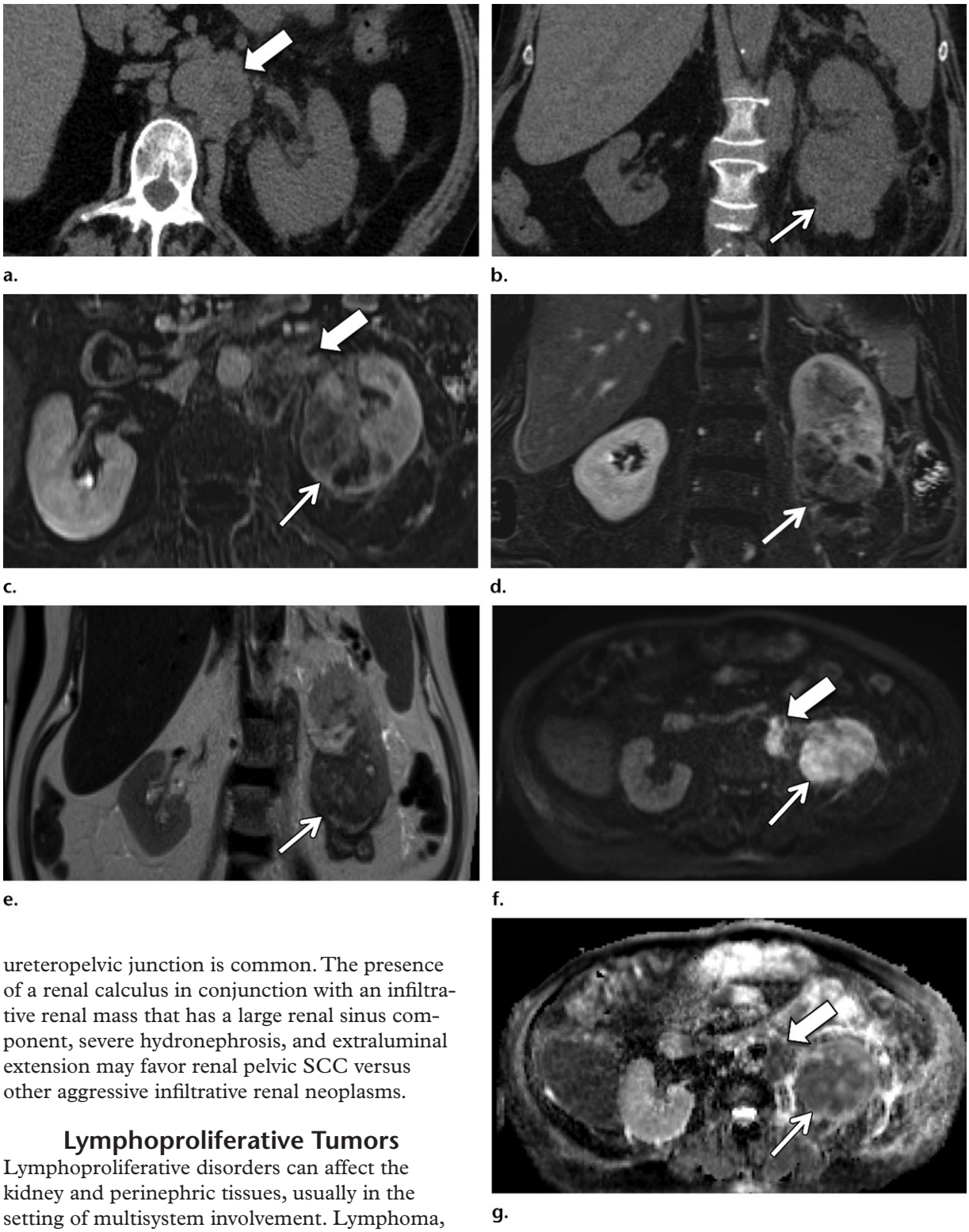

ureteropelvic junction is common. The presence of a renal calculus in conjunction with an infiltrative renal mass that has a large renal sinus component, severe hydronephrosis, and extraluminal extension may favor renal pelvic SCC versus other aggressive infiltrative renal neoplasms.

Lymphoproliferative Tumors

Lymphoproliferative disorders can affect the kidney and perinephric tissues, usually in the setting of multisystem involvement. Lymphoma, leukemia, and plasmacytoma can exhibit infiltrative growth, commonly manifesting as multiple parenchymal or perinephric masses.

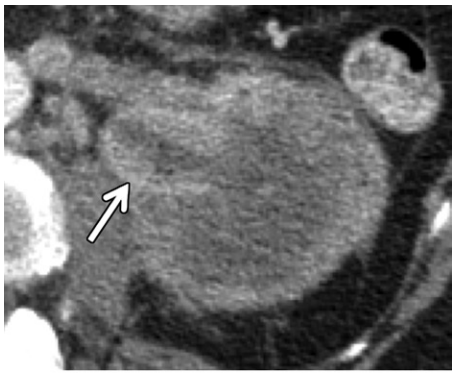

a.

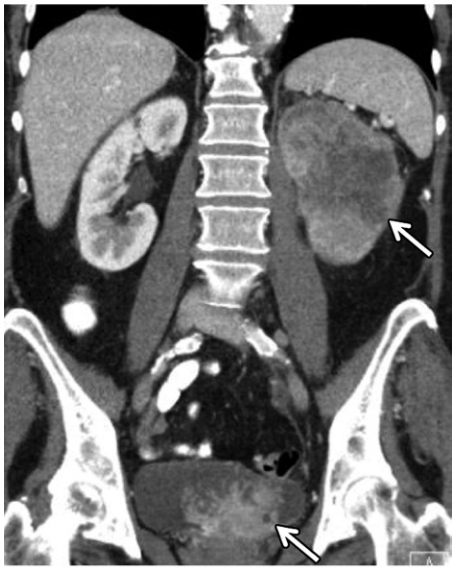

b.

Figure 14. Synchronous upper- and lower-tract UCCs in an 86-year-old woman with left flank pain that worsened over 4–6 weeks. **(a)** Axial contrast-enhanced CT image shows an infiltrative left renal mass (arrow) with relative preservation of the renal contour, obliteration of the sinus fat, and markedly irregular urothelial thickening of the renal pelvis. **(b)** Coronal contrast-enhanced CT image shows a synchronous mass in the urinary bladder (arrows). The axial contrast-enhanced CT image in Figure E2 shows the frondlike bladder mass extending from the posterior wall.

Renal Lymphoma

Lymphoma encompasses a heterogeneous group of neoplasms characterized by the expansion of abnormal lymphoid cells. While this may occur in any organ, it most commonly involves the lymph nodes. The World Health Organization has classified more than 70 distinct subtypes according to the derived cell type, but informally these types are broadly distinguished as Hodgkin and non-Hodgkin lymphomas. Although any subtype of lymphoma can involve the kidneys, renal lymphoma is most commonly seen in patients with non-Hodgkin lymphoma (usually B-cell or Burkitt lymphoma subtypes).

Because the kidneys lack any substantial lymphoid tissue, lymphoma rarely involves the kidneys as a primary process without evidence of disease elsewhere. Most cases of renal lymphoma occur in the presence of widespread nodal or extranodal disease, with secondary spread to the kidney via hematogenous dissemination or contiguous extension of retroperitoneal disease. After the hematopoietic and reticuloendothelial organs, the kidneys are the next most common site affected by extranodal spread of lymphoma (47). Lymphomatous spread to the kidneys is usually clinically silent and occurs late in the course of the disease, after the diagnosis has been established.

Only in rare cases is renal lymphoma the initial or even predominant disease manifestation (48). Autopsy series have reported renal involvement in 30%–60% of patients with lymphoma, but only 3%–8% of patients have detectable renal abnormalities at imaging during the course of therapy (47,49–52). This large discrepancy between radiologic and histopathologic detection rates may be at least partially attributable to the often asymptomatic and microscopic nature of renal lymphoma and the older generation of CT scanners used in these studies. Renal lymphoma is predominantly a bilateral process, found to involve both kidneys in nearly 75% of cases (47).

Renal lymphoma has a variety of imaging patterns that relate to its variable mechanisms of spread and growth. Malignant lymphocytes that reach the renal parenchyma through hematogenous spread proliferate within the interstitium and can exhibit both expansile and infiltrative patterns of growth. Most cases (50%–60%) form multiple bilateral focal masses or, less commonly (10%–25%), a single mass (47). The masses are usually circumscribed, but they may have partially infiltrative margins (Fig 16). At US, lymphomatous masses are hypoechoic and homogeneous. Use of contrast material at CT is essential for lymphoma detection, as many of these masses are small with little cortical deformity. Focal lymphomatous deposits on CT images are homogeneous masses that enhance less than the normal renal parenchyma. Large masses tend to be more heterogeneous.

Alternatively, malignant lymphocytes may diffusely infiltrate the renal interstitium, with the underlying nephrons, collecting ducts, and blood vessels used to provide a framework for tumor growth (Figs 16, 17). This pattern of diffuse lymphomatous infiltration (20% of cases), which is almost always bilateral, manifests with irregular tumor margins and global renal enlargement without contour disruption (48,51). Extension beyond the kidney is common and may include invasion of the perinephric space

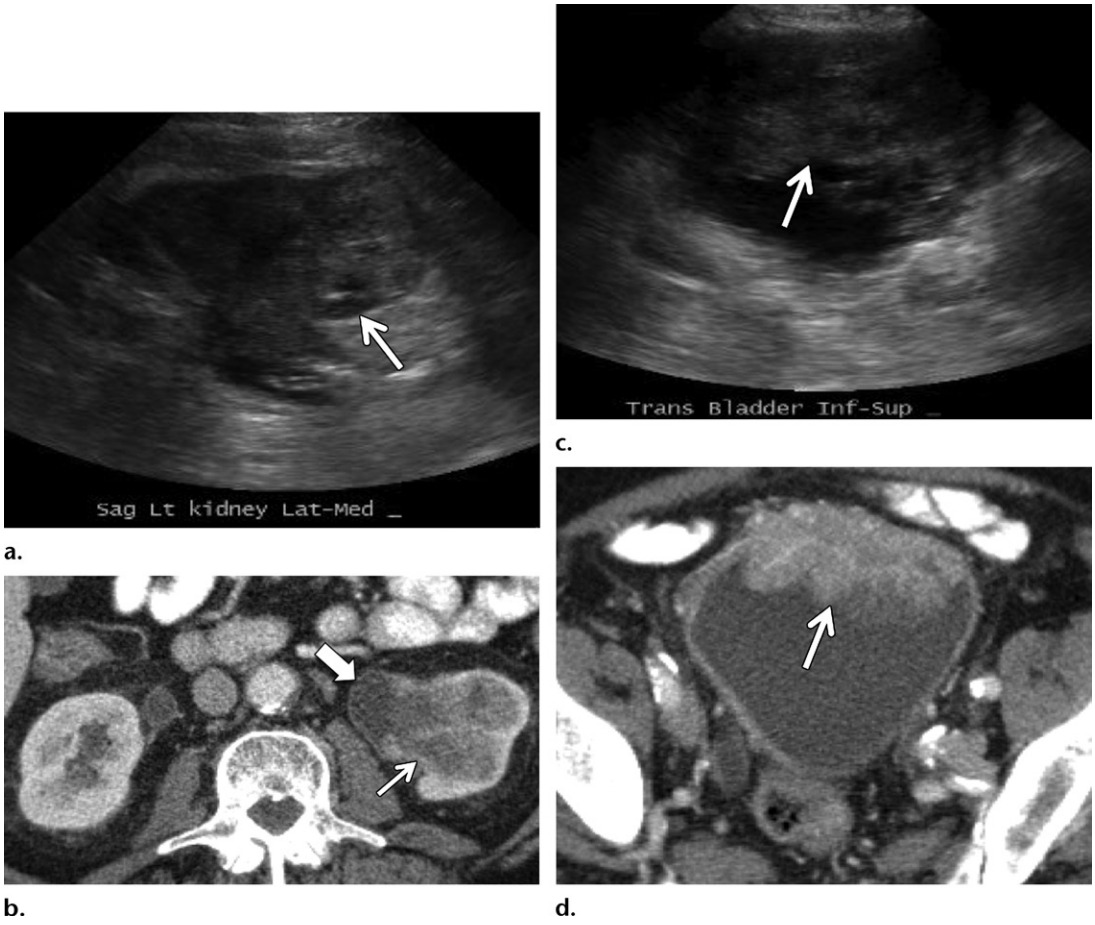

Figure 15. Metachronous upper- and lower-tract UCCs in an 81-year-old man with a history of bladder UCC resection. **(a, b)** Sagittal gray-scale US **(a)** and axial contrast-enhanced CT **(b)** images show an infiltrative mass (thin arrow) replacing the left interpolar and lower pole calyces and extending to the renal pelvis, with moderate hydroureteronephrosis (thick arrow in **b**). *Lat - Med* = lateromedial. **(c, d)** Transverse US **(c)** and axial contrast-enhanced CT **(d)** images show a recurrent multilobulated mass (arrow) arising from the anterior bladder wall.

and encasement of the ureter and vascular pedicle. In most patients, the collecting system and renal vasculature remain patent; this is a characteristic feature of lymphoma. The US appearance of diffuse lymphomatous infiltration can be subtle and includes heterogeneous echogenicity of the parenchyma in an enlarged kidney, with loss of the normal echogenic renal sinus fat. Bilateral nephromegaly may be the only detectable feature at noncontrast CT. Contrast enhancement will demonstrate replacement of the parenchyma by a confluent poorly marginated hypoenhancing mass, with loss of the normal corticomedullary differentiation.

Direct renal invasion from contiguous retroperitoneal disease is another common (25%–30% of cases) pattern of lymphomatous spread (Fig 18). Affected patients usually have widespread disease with bulky tumors. At imaging, large retroperitoneal disease can be seen infiltrating the kidneys and perinephric space. The renal sinus fat is invaded, with encasement of the collecting system and renal vessels.

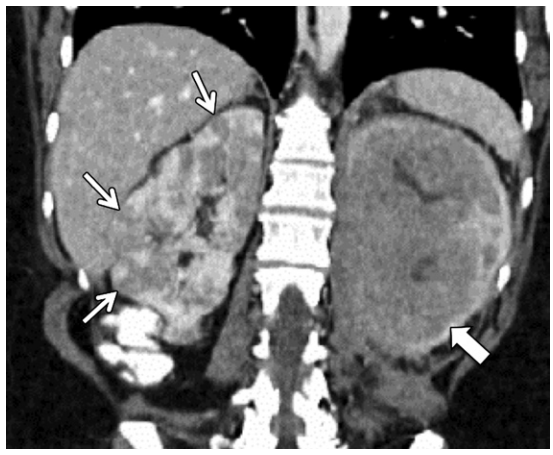

Figure 16. Renal lymphoma, diffusely infiltrative and multinodular. Coronal contrast-enhanced CT image shows a diffusely infiltrative mass (thick arrow) in the left kidney and multifocal nodular masses (thin arrows) with partially infiltrative margins in the right kidney.

Renal lymphoma has multiple imaging appearances related to its variable growth pattern (infiltrative or expansile), mechanism of spread

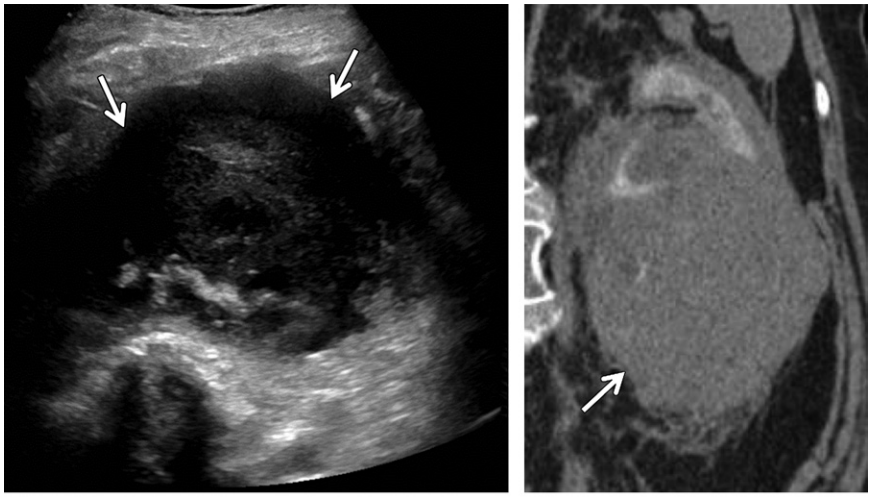

a. b.

Figure 17. Aggressive diffuse large B-cell lymphoma in an 83-year-old woman with acute kidney injury. **(a)** Initial sagittal US image shows a hypoechoic mass (arrows) infiltrating the left kidney. **(b)** Subsequent coronal contrast-enhanced CT image shows an infiltrative soft-tissue mass (arrow) replacing most of the renal parenchyma and invading the perinephric space.

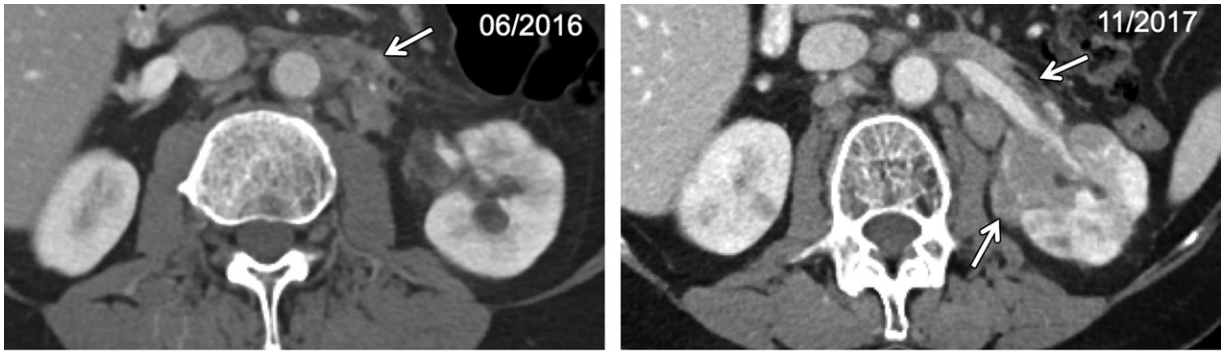

a. b.

c.

Figure 18. Direct renal invasion by contiguous retroperitoneal lymphoma. **(a)** Axial contrast-enhanced CT image shows retroperitoneal infiltrative soft tissue (arrow), indicating confluent lymphadenopathy. **(b)** Follow-up axial contrast-enhanced CT image shows interval extension of retroperitoneal disease into the left renal sinus and renal parenchyma (arrows). **(c)** Additional follow-up axial contrast-enhanced CT image shows that new multifocal infiltrative lymphomatous involvement of the right kidney (arrow) also is present.

(hematogenous or direct extension), and extent of perinephric invasion. The combination of infiltrative renal masses in the presence of bulky perinephric disease, widespread lymphadenopathy, splenomegaly, and bilateral involvement is suggestive of lymphoma. In many cases, patients have an established diagnosis of lymphoma at the time of imaging.

Renal Leukemia

Leukemia represents a diverse group of malignant hematopoietic precursor cells that originate in and infiltrate the bone marrow. The classification of leukemia is based on the clonal expansion of either immature lymphoblasts (acute leukemia) or mature lymphocytes (chronic leukemia), which are further subdivided according to their cell lineage. Although most cases occur in adults, leukemia is the most common pediatric malignancy, with acute lymphocytic leukemia constituting approximately 75% of childhood cases (53). Leukemia is not limited to the peripheral blood and hematopoietic organs (spleen, liver, and lymph nodes), as autopsy series have identified infiltration of the kidneys in 60%–90% of cases (54,55). Despite the high prevalence of renal involvement at autopsy, only up to 5% of patients have identifiable leukemic renal disease at imaging; this is an even greater discrepancy than that found with renal lymphoma (56). However, accurate radiologic assessment of renal

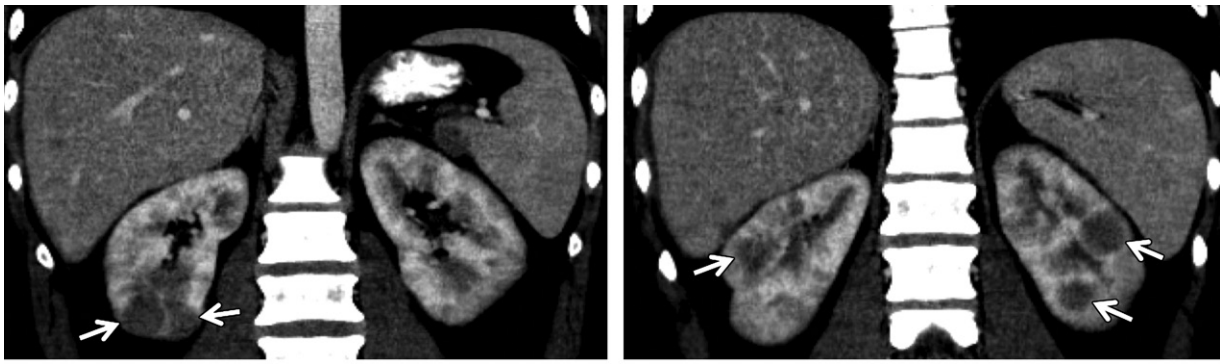

a. b.

Figure 19. Renal involvement in a 31-year-old man with acute lymphoblastic leukemia. Coronal contrast-enhanced CT images obtained at different levels show mild nephromegaly with multifocal bilateral low-attenuation leukemic nodules (arrows). CT also depicted splenomegaly (Fig E3) in this patient.

leukemia is limited, as cross-sectional imaging is not routinely performed and renal involvement is usually asymptomatic.

Leukemic involvement of the kidney most commonly manifests as nephromegaly from diffuse or focal infiltration of leukemic cells. This is usually a bilateral and relatively symmetric process, although unilateral and bilateral asymmetric infiltration can occur. At CT, diffuse infiltration manifests as a markedly enlarged kidney with homogeneous low attenuation and loss of normal corticomedullary differentiation. More focal leukemic deposits appear on CT images as rounded low-attenuation masses (single or multiple) or wedge-shaped and geographic ill-defined regions of low attenuation, enhancing less than the surrounding normal parenchyma after contrast material administration (Fig 19). On US images, the kidneys are enlarged, with diffuse or multifocal regions of decreased parenchymal echogenicity (56–58).

Renal Plasmacytoma

Neoplastic proliferation of plasma cells occurs primarily in bone marrow as either multiple tumors (multiple myeloma) or a solitary tumor (solitary bone plasmacytoma). Plasma cell tumors that occur outside of the bone marrow (extramedullary plasmacytomas) are rare, accounting for only 3%–7% of all plasma cell tumors. Patients diagnosed with this condition are usually aged 50–70 years, and the incidence is three times higher in men. The upper respiratory tract is the most frequent (in up to 85% of cases) extramedullary tumor location, but tumors can occur in almost any organ (59–61). Rarely, extramedullary plasmacytomas can involve the kidney, appearing as an infiltrative mass that extends into the perirenal fat. The diagnosis of plasmacytoma is contingent on establishing a monoclonal plasma cell tumor in an extramedullary site and without multiple myeloma identified on imaging, blood, or urine studies (eg, presence of anemia, hypercalcemia, renal insufficiency, and Bence Jones protein in the urine). Imaging and clinical features cannot reliably distinguish an extramedullary plasmacytoma from other infiltrative renal masses; pathologic diagnosis is generally necessary (59–61).

Renal Metastases

In autopsy series (62,63), the incidence of metastasis to the kidney has ranged from 7% to 13%. With advances in oncologic care leading to prolonged patient survival and with increasing use of surveillance cross-sectional imaging, renal metastases are now frequently detected in living patients, whereas historically they were typically identified postmortem (64). However, the prevalence of kidney metastasis detected at imaging in living patients has been observed to be closer to 1% (65). Lung cancer is the most common primary malignancy to metastasize to the kidneys, accounting for up to 44% of metastases (Fig 20), followed by colorectal, stomach, and breast malignancies (Fig 21) (62–64,66). Metastases from other primary tumors are much less common (Fig 22). The diagnosis of metastasis to the kidney in patients without evidence of a widespread nonrenal malignancy is rare; a focal renal mass is more likely to represent a primary renal tumor (67).

Renal metastases have a wide spectrum of imaging characteristics that largely depend on the site of the primary tumor. Most metastases form multifocal small round discrete masses, although infiltrative growth with irregular margins has been reported in up to 28% of cases (68,69). Multifocal bilateral masses are more common than unilateral solitary and bilateral solitary masses. They are often homogeneous and hypoenhancing relative to the normal renal parenchyma on contrast-enhanced images, but heterogeneous features, including areas of cystic necrosis, hemorrhage, calcification, and hypervascularity, have

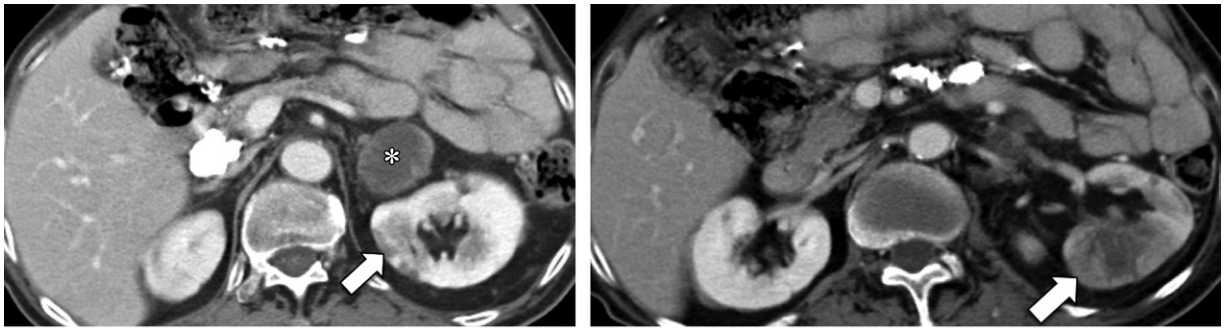

a. b.

Figure 20. Renal metastases in a 75-year-old man with non–small cell lung cancer. Axial contrast-enhanced CT images show developing infiltrative left upper and lower pole renal metastases (arrow) and necrotic left adrenal metastasis (* in **a**). Additional images obtained in this patient (Fig E4) show the non–small cell lung cancer, as well as ring-enhancing brain metastases.

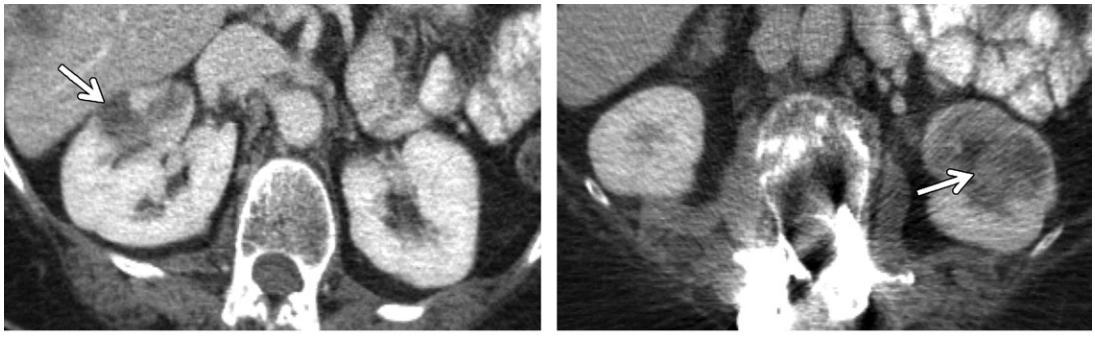

a. b.

Figure 21. Renal metastases in a 64-year-old woman with left breast cancer. Axial contrast-enhanced CT images show bilateral infiltrative renal metastases involving the right anterior interpolar region (arrow in **a**) and left lower pole (arrow in **b**). The CT images in Figure E5 show lung and liver metastases in this patient.

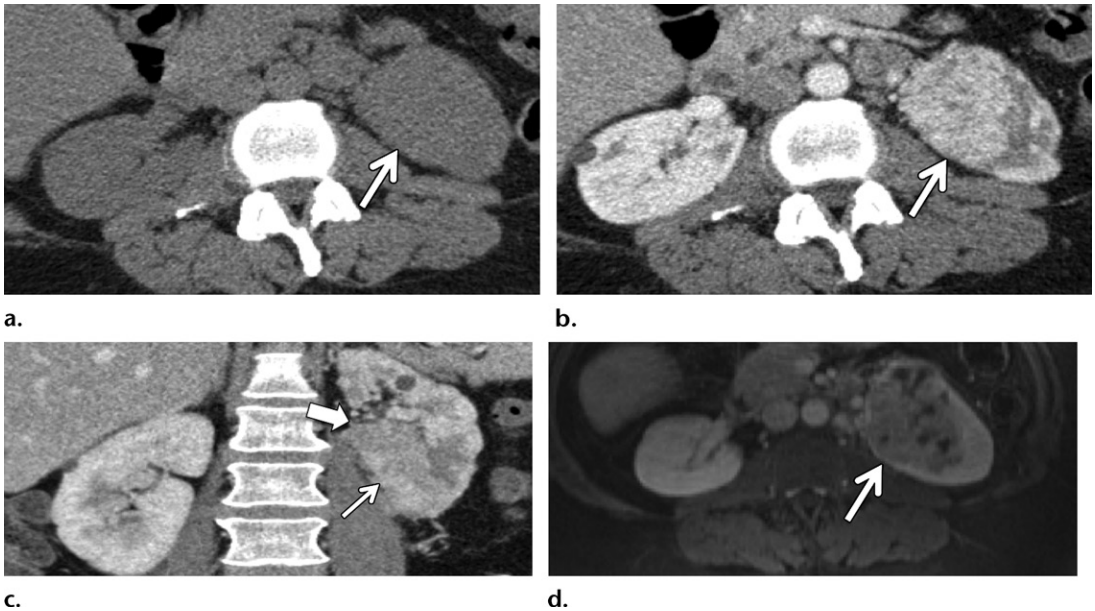

a. b.

c. d.

Figure 22. Renal metastases in a 55-year-old man with papillary thyroid carcinoma, hematuria, and left flank pain. **(a)** On an axial noncontrast CT image of the left kidney (arrow), no renal metastasis is detectable. **(b–d)** Follow-up axial **(b)** and coronal **(c)** contrast-enhanced CT images and contrast-enhanced T1-weighted MR image **(d)** show an infiltrative heterogeneously enhancing left renal metastasis (thin arrow) with renal sinus invasion (thick arrow in **c**). Figure E6 shows additional enhancing liver metastases in this patient.

been described. Invasion of the renal vein and inferior vena cava is uncommon (68,69). Larger masses often infiltrate the perinephric space; this occurrence is associated with primary lung and melanoma tumors (68–70). Large and exophytic renal metastases, usually an uncommon appearance for metastases, are characteristic of primary colon cancer (69).

Given the relatively low frequency of primary infiltrative renal neoplasms, an infiltrative renal mass in a patient with disseminated nonrenal malignancy most likely represents metastatic disease. However, a definitive diagnosis requires tissue sampling.

Infiltrative Mimics of Malignancy

An infiltrative pattern at imaging typically implies the presence of an aggressive malignancy. However, there are inflammatory, autoimmune, vascular, and other nonmalignant processes with patterns that may mimic the pattern of an infiltrative tumor.

Acute Bacterial Pyelonephritis

Pyelonephritis manifests in many forms, including acute and bacterial, or chronic and xanthogranulomatous. Urinary tract infections typically begin in the bladder and involve the kidneys by way of direct extension or, much less commonly, hematogenous spread. Involvement of the renal parenchyma causes a tubulointerstitial inflammatory reaction that results in the imaging appearance of pyelonephritis (71). Acute bacterial pyelonephritis, which occurs up to twice as often in women, is most commonly caused by *Escherichia coli* and is typically accompanied by the clinical symptoms of flank pain and fever, and lower urinary tract symptoms such as dysuria (72).

The diagnosis of bacterial pyelonephritis is confirmed with urinalysis and/or urine culture, and the infection is treated with antibiotics. As such, imaging typically does not have a role in the diagnosis of uncomplicated urinary tract infections and should instead be reserved for cases with an unclear clinical picture or for patients with diabetes, infections that do not respond to antibiotics, suspected anatomic abnormality, or suspected complications such as abscess.

Initial imaging for acute bacterial pyelonephritis often begins with US, although the sensitivity of this modality is low. Gray-scale US typically depicts acute pyelonephritis as focal wedge-shaped areas of increased or decreased echogenicity with poor corticomedullary differentiation. On color and power Doppler US images, there may be corresponding areas of decreased vascularity. In addition, nephric or perinephric edema may be present, or a perinephric abscess may be detected in complicated cases. The sensitivity of gray-scale US for the detection of acute pyelonephritis ranges from 11% to 40%, which improves to 63% with the use of Doppler imaging (73). Negative results at conventional US do not preclude the diagnosis of acute pyelonephritis. Contrast-enhanced US offers greater sensitivity for acute pyelonephritis owing to the improved detection of parenchymal hypoperfusion that occurs as a result of the focal vasoconstriction and vascular compression caused by the inflammation (73). However, no specific recommendations regarding contrast-enhanced US for imaging of acute pyelonephritis are provided in the 2018 American College of Radiology Appropriateness Criteria, as further study of this modality for this purpose is needed (74).

Contrast-enhanced CT is the imaging modality of choice for the evaluation of pyelonephritis, as it has higher sensitivity (87%) for the detection of pyelonephritis and other urinary tract abnormalities such as nephrolithiasis, hydronephrosis, and perinephric abscess (75). Portal venous phase CT images may show a wedge-shaped pattern of infiltration, manifesting as parenchymal hypoperfusion or a striated nephrogram appearance (Fig 23). MRI, which is most commonly used only in special populations such as children and pregnant patients, also may show wedge-shaped or striated nephrogram patterns of parenchymal hypoenhancement. Markedly restricted diffusion and T2-weighted hyperintensity may be seen in the affected areas. Although the findings of pyelonephritis are usually unilateral, they can be bilateral. Imaging-depicted abnormalities resolve within 1–5 months after appropriate antibiotic treatment, which can help distinguish cases where an infiltrative malignant mass is under consideration (76).

Xanthogranulomatous Pyelonephritis

Xanthogranulomatous pyelonephritis (XGP) is a chronic destructive granulomatous process that results from chronic or recurrent urinary tract infection, most commonly with *Proteus mirabilis* or *E coli* bacteria. XGP is uncommon, accounting for approximately 0.6% of histologically documented cases of pyelonephritis (77). This condition is more common in women and typically manifests as fever, flank or abdominal pain, and a palpable mass (77). XGP is an important diagnosis to recognize, as a delayed diagnosis can lead to complete destruction of the kidney and injury to adjacent organs and viscera, such as involvement of the psoas muscle or development of a gastrointestinal fistula. The treatment of XGP is nephrectomy, with conservative nephron-sparing approaches appropriate only in cases with focal involvement.

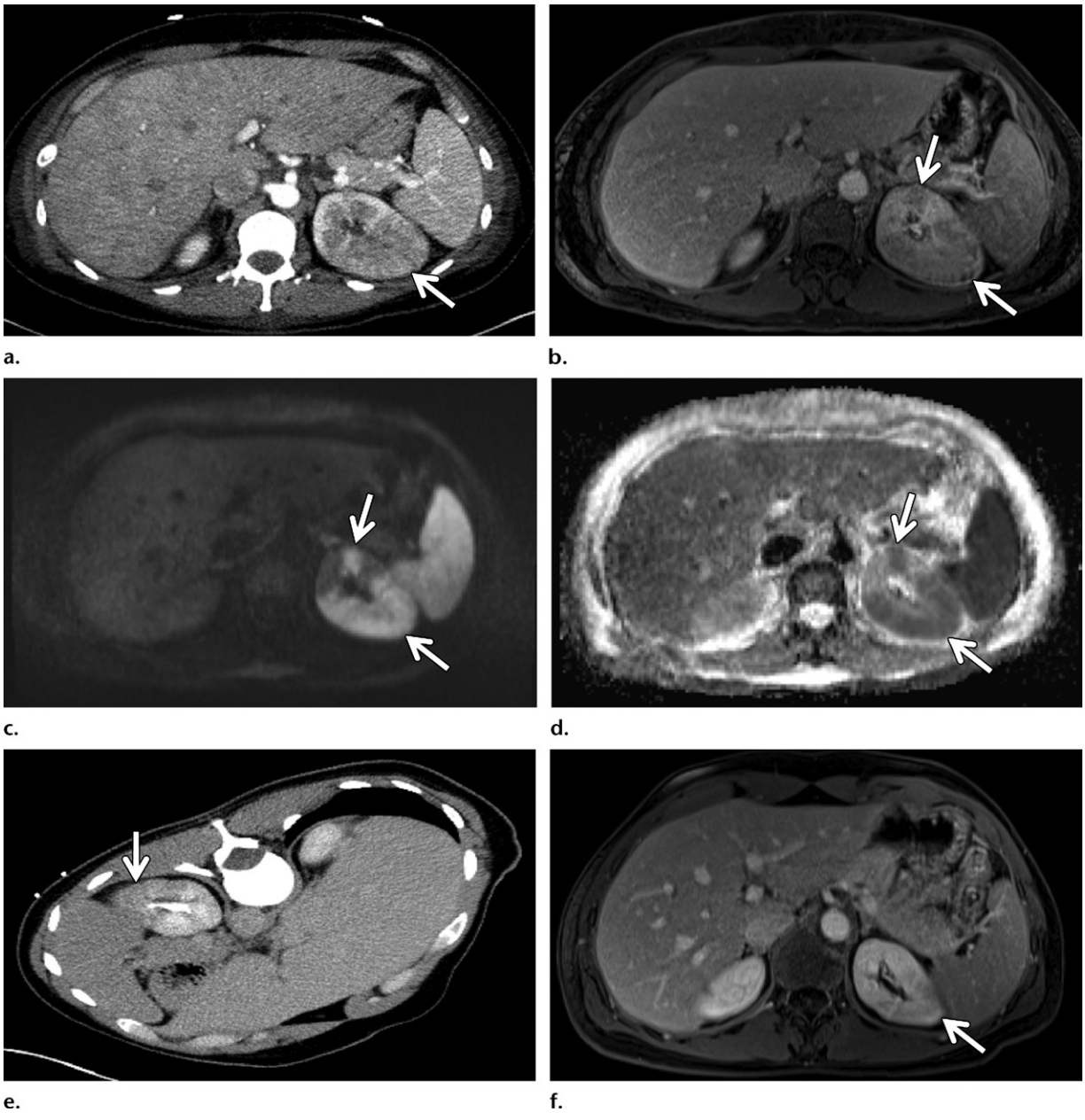

Figure 23. Pyelonephritis in a 36-year-old woman with intermittent fevers and weight loss. **(a)** Axial contrast-enhanced CT image shows a poorly marginated wedge-shaped area of heterogeneously decreased enhancement (arrow) in the left upper pole. **(b–d)** Axial contrast-enhanced T1-weighted MR image obtained the following day **(b)** shows similar areas of decreased enhancement (arrows in **b**), compared with the normal parenchyma in the left upper pole, with increased signal intensity (arrows in **c**) on the axial diffusion-weighted MR image **(c)** and decreased signal intensity (arrows in **d**) on the corresponding apparent diffusion coefficient map **(d)**, indicating restricted diffusion. Biopsy was planned for 1 month later to rule out infiltrative renal tumor but was canceled after intraprocedural contrast-enhanced CT (with the patient in the prone position) **(e)** revealed an interval decrease in geographic hypoenhancement (arrow in **e**), indicating a resolving infectious-inflammatory process. **(f)** Follow-up axial contrast-enhanced fat-suppressed T1-weighted MR image shows expected continued improved parenchymal hypoenhancement (arrow), consistent with resolving pyelonephritis.

At imaging, XGP is characterized by reniform enlargement of the kidney, with poorly marginated parenchymal abnormalities that correspond to areas of inflammation that may extend into the perinephric spaces (Fig 24). This ill-defined infiltrative pattern can be mistaken for infiltrative malignancy, especially in cases of focal XGP. There is typically marked dilatation of the calyces and cortical thinning with central obstructing calculi, often with staghorn morphology. The majority of cases (73%–100%) have an associated renal calculus (either calyceal or staghorn) (77,78). In one study (77), the classic "bear paw" appearance was present in only 23% of cases.

Renal Infarct

Renal infarcts can arise from a number of processes such as thromboembolism, vasculitis,

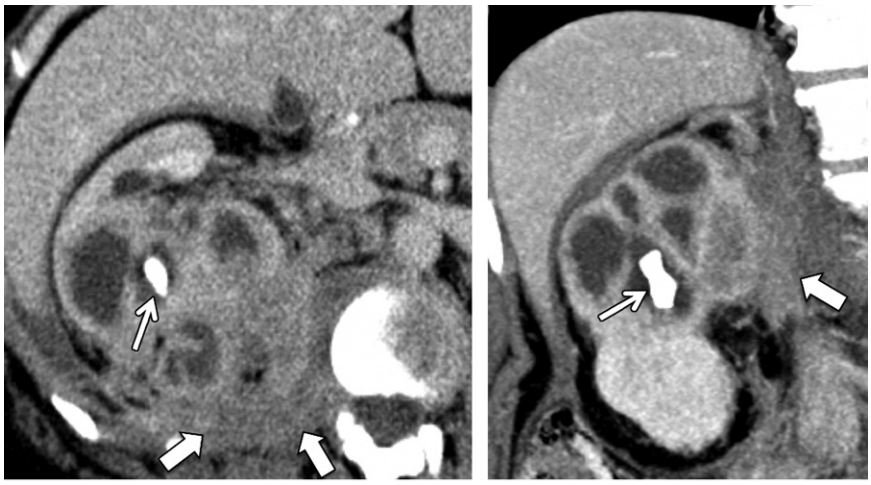

a. b.

Figure 24. Xanthogranulomatous pyelonephritis confirmed after nephrectomy in a 44-year-old woman. Axial **(a)** and coronal **(b)** contrast-enhanced CT images show a large centrally located calculus (thin arrow) and thinned parenchyma, with a bear paw appearance of radially arrayed dilated calyces and extensive ill-defined infiltrative soft tissue (thick arrows) in the perinephric space.

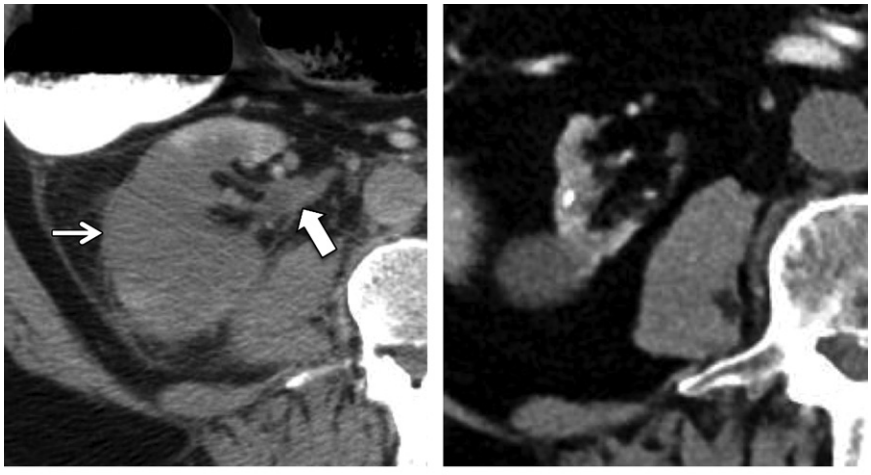

a. b.

Figure 25. Renal infarct in a 67-year-old man with atrial fibrillation who was evaluated for acute cardioembolic stroke. **(a)** Axial contrast-enhanced CT image of the right kidney shows a large wedge-shaped area of parenchymal nonenhancement (thin arrow) that appears mildly expanded secondary to a renal artery thrombus (thick arrow). **(b)** Follow-up axial contrast-enhanced CT image obtained several years later shows evolution of the infarct, with parenchymal atrophy and contour deformity.

and trauma, but most of them commonly occur secondary to cardiovascular disease (79). The imaging appearance of an infarct depends on the territories of vascular compromise and extent of associated parenchymal involvement. For example, thrombosis of a small vessel may cause a segmental infarct and resultant focal wedge-shaped areas of apparent infiltration secondary to hypoperfusion (Fig 25). On the other hand, occlusion of the renal artery will cause a global insult. Such an infarct may appear as an enlarged kidney with preserved reniform shape. The renal parenchyma will appear diffusely infiltrated and hypoenhancing, with preserved enhancement in a subcapsular rim owing to perfusion from capsular arteries that arise as early branches from the renal artery (cortical rim sign) (80). When present, this unique feature can be useful in distinguishing infarct from pyelonephritis. At follow-up imaging, the infarcted segments will often demonstrate parenchymal volume loss and persistent hypoenhancement.

IgG4–related Kidney Disease

Immunoglobulin G4 (IgG4)–related disease is an immune-mediated systemic disease that can af-

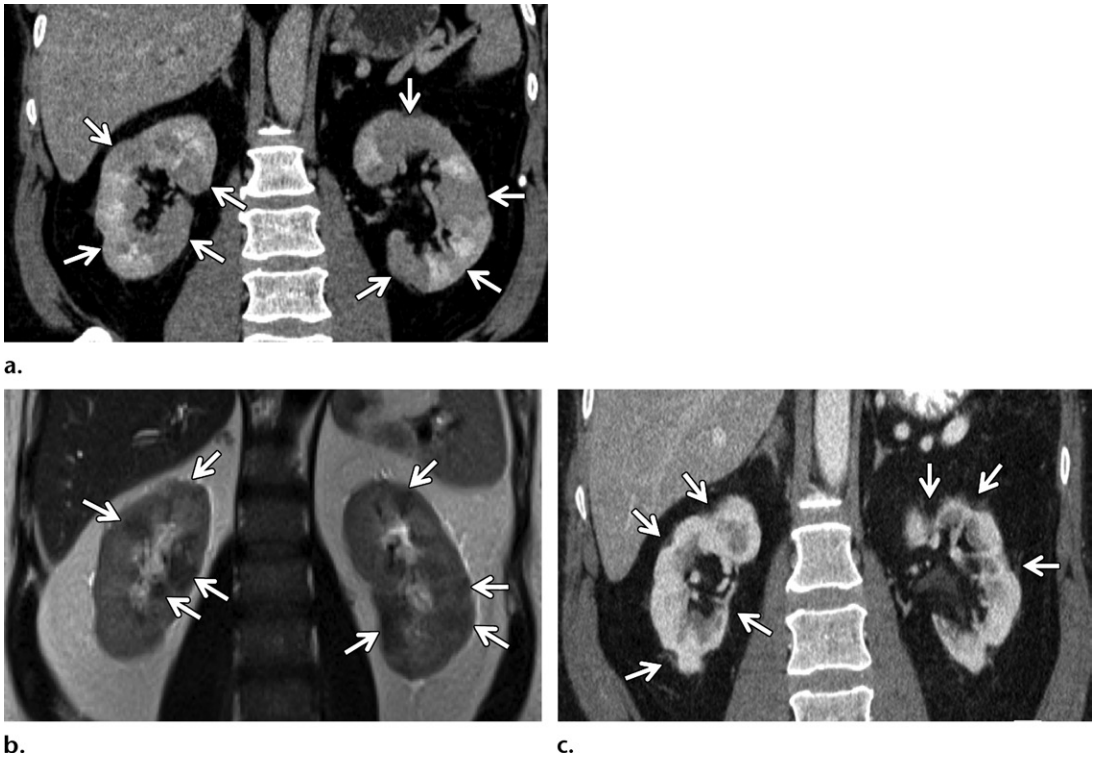

Figure 26. IgG4-RKD in a 56-year-old man with autoimmune pancreatitis and sclerosing cholangitis. **(a)** Coronal contrast-enhanced CT image shows multiple regions of patchy infiltrative low-attenuation lesions (arrows) in both kidneys. **(b)** Coronal T2-weighted MR image shows low signal intensity (arrows) in the regions of parenchymal infiltration. **(c)** Coronal contrast-enhanced posttreatment CT image shows resolution of the parenchymal lesions, with multifocal scarring (arrows).

fect nearly every organ. The pancreas is the most common organ to be affected, and up to 35% of patients who develop autoimmune pancreatitis have renal involvement, referred to as IgG4-related kidney disease (IgG4-RKD) (81). Isolated IgG4-RKD without other organ involvement is rare. The most common histologic features of IgG4-RKD are tubulointerstitial nephritis with lymphoplasmacytic infiltration, increased IgG4-positive plasma cells, and fibrosis. IgG4-RKD usually responds well to steroids, but if not treated, it can progress to irreversible renal failure.

There are several imaging patterns of IgG4-RKD parenchymal involvement, including a single nodule, multiple nodules, and diffuse patchy infiltrative lesions (Fig 26) (81). The nodules are rounded or wedge shaped and can have ill-defined margins. The most common appearance is that of multiple small nodules in both kidneys, predominantly in the renal cortex. Renal lesions in IgG4-RKD usually are not visible on noncontrast CT images. On contrast-enhanced CT images, the renal parenchymal lesions have low attenuation relative to the normal parenchyma. At MRI, the lesions are often hypointense on T2-weighted images and isointense on noncontrast T1-weighted images and demonstrate mild progressive enhancement on contrast-enhanced T1-weighted images. Diffusion-weighted MR images show a hyperintense signal with hypointensity on the corresponding apparent diffusion coefficient map, which has been reported as useful for the detection of IgG4-RKD (82). The renal lesions typically resolve after the initiation of treatment, although regions of scarlike focal cortical atrophy can occur (83). The radiologic differentiation of IgG4-RKD from lymphoma, metastases, pyelonephritis, infarct, or primary renal tumor can be difficult, and the presence of concomitant pancreatic or biliary involvement (the most commonly involved organs) can help suggest the diagnosis of IgG4-RKD.

Conclusion

Infiltrative renal malignancies are a diverse subset of renal lesions characterized by an ill-defined margin between the mass and the normal renal parenchyma. Infiltrative renal malignancies are often more aggressive and confer a worse prognosis compared with more well-defined neoplasms such as conventional RCC (Table 2). However, other causes such as infectious, vascular, and autoimmune processes also can have an infiltrative appearance at imaging (Table 3). As such, it is important to correlate imaging findings with the patient history and

Table 2: Distinguishing Features of Infiltrative Renal Malignancies

Tumor Origin Type	Tumor Subtype	Distinguishing Features
Renal cortical	RCC with atypical growth pattern	Most RCCs have expansile growth; however, atypical RCCs, given their high overall frequency, should be considered in cases of infiltrative renal masses
	RCC with sarcomatoid or rhabdoid differentiation	Any conventional RCC subtype with sarcomatoid or rhabdoid differentiation usually exhibits infiltrative growth When present, a disrupted pseudocapsule with an invasive margin, peritumoral neovascularity, and larger peritumoral vessel size are more commonly associated with RCCs that have sarcomatoid features
Renal medullary	Renal medullary carcinoma	Renal medullary carcinoma is an aggressive tumor that occurs almost exclusively in young African Americans with the sickle cell trait
Renal pelvic	Renal UCC	Eight percent of UCCs occur in the kidney and are centered in the renal pelvis Commonly involve metachronous spread from more frequent bladder UCC
Lymphoproliferative	Renal lymphoma	Bulky perinephric disease, widespread lymphadenopathy, splenomegaly, and bilateral renal involvement are suggestive of lymphoma
Metastatic	Renal metastases	New infiltrative renal mass with history of extrarenal cancer most likely represents metastatic disease Lung cancer is the most common primary source

Table 3: Distinguishing Features of Processes That Mimic Infiltrative Renal Malignancy

Nonmalignant Infiltrative Process	Cause	Distinguishing Features
Acute bacterial pyelonephritis	Infectious-inflammatory	Fever, chills, flank pain, and pyuria can help distinguish infectious causes In the absence of clinically suspected pyelonephritis, expected interval improvement of imaging abnormalities (1–5 months) with appropriate antibiotic treatment can help differentiate acute bacterial pyelonephritis from an infiltrative malignancy
Xanthogranulomatous pyelonephritis	Infectious-inflammatory	Recurrent urinary tract infections, fever, and flank pain in a woman can clinically raise suspicion for a chronic infectious process Process is most commonly unilateral, with diffuse renal involvement Nearly all cases involve an associated renal calculus (often staghorn morphology), and the classic bear paw appearance is present in nearly 25% of cases
Renal infarct	Ischemic	Majority of cases are due to thromboembolic phenomena, and patients often have a history of atrial fibrillation, valvular heart disease, or myocardial infarction When present, a thin rim of subcapsular cortex (ie, cortical rim sign) can be useful in distinguishing infarct from other infiltrative processes
IgG4-RKD	Autoimmune mediated	Isolated IgG4-RKD without other organ involvement is rare, and the presence of concomitant retroperitoneal, and pancreatic or biliary involvement (most commonly involved organs) can help suggest the diagnosis of IgG4-RKD

corresponding laboratory results. The radiologist should carefully consider these mimicking processes while evaluating the kidney, as they can easily be mistaken for infiltrative masses, resulting in the patient undergoing unnecessary surgery.

References

1. Pickhardt PJ, Lonergan GJ, Davis CJ Jr, Kashitani N, Wagner BJ. From the archives of the AFIP: infiltrative renal lesions—radiologic-pathologic correlation. Armed Forces Institute of Pathology. RadioGraphics 2000;20(1):215–243.
2. Zagoria RJ, Wolfman NT, Karstaedt N, Hinn GC, Dyer RB, Chen YM. CT features of renal cell carcinoma with emphasis on relation to tumor size. Invest Radiol 1990;25(3):261–266.

3. Hartman DS, Davidson AJ, Davis CJ Jr, Goldman SM. Infiltrative renal lesions: CT-sonographic-pathologic correlation. AJR Am J Roentgenol 1988;150(5):1061–1064.
4. Wang Y, Tanaka H, Ye Y, et al. The complete spectrum of infiltrative renal masses: clinical characteristics and prognostic implications. Urology 2019;130:86–92.
5. Tanaka H, Ding X, Ye Y, et al. Infiltrative renal masses: clinical significance and fidelity of documentation. Eur Urol Oncol 2019. 10.1016/j.euo.2019.07.015. Published online August 20, 2019.
6. Nishikimi T, Tsuzuki T, Fujita T, et al. The postoperative pathological prognostic parameters of clear cell renal cell carcinoma in pT1a cases. Pathol Int 2011;61(3):116–121.
7. Expert Panel on Urological Imaging; Wolfman DJ, Marko J, Nikolaidis P, et al. ACR appropriateness criteria: hematuria. American College of Radiology website https://acsearch.acr.org/docs/69490/Narrative. Revised 2019. Accessed April 13, 2020.
8. Ignee A, Straub B, Schuessler G, Dietrich CF. Contrast enhanced ultrasound of renal masses. World J Radiol 2010;2(1):15–31.
9. Barr RG, Peterson C, Hindi A. Evaluation of indeterminate renal masses with contrast-enhanced US: a diagnostic performance study. Radiology 2014;271(1):133–142.
10. Wang ZJ, Nikolaidis P, Khatri G, et al. ACR Appropriateness criteria indeterminate renal mass. American College of Radiology website. https://acsearch.acr.org/docs/69367/Narrative/. Accessed April 23, 2020.
11. Kim JH, Sun HY, Hwang J, et al. Diagnostic accuracy of contrast-enhanced computed tomography and contrast-enhanced magnetic resonance imaging of small renal masses in real practice: sensitivity and specificity according to subjective radiologic interpretation. World J Surg Oncol 2016;14(1):260.
12. Kwon T, Jeong IG, Yoo S, et al. Role of MRI in indeterminate renal mass: diagnostic accuracy and impact on clinical decision making. Int Urol Nephrol 2015;47(4):585–593.
13. Fukatsu A, Tsuzuki T, Sassa N, et al. Growth pattern, an important pathologic prognostic parameter for clear cell renal cell carcinoma. Am J Clin Pathol 2013;140(4):500–505.
14. Hu EM, Zhang A, Silverman SG, et al. Multi-institutional analysis of CT and MRI reports evaluating indeterminate renal masses: comparison to a national survey investigating desired report elements. Abdom Radiol (NY) 2018;43(12):3493–3502. [Published correction appears in Abdom Radiol (NY) 2018;43(11):3206.]
15. Davenport MS, Hu EM, Zhang A, et al. Standardized report template for indeterminate renal masses at CT and MRI: a collaborative product of the SAR Disease-Focused Panel on Renal Cell Carcinoma. Abdom Radiol (NY) 2019;44(4):1423–1429.
16. Delahunt B, Cheville JC, Martignoni G, et al. The International Society of Urological Pathology (ISUP) grading system for renal cell carcinoma and other prognostic parameters. Am J Surg Pathol 2013;37(10):1490–1504.
17. Moch H, Cubilla AL, Humphrey PA, Reuter VE, Ulbright TM. The 2016 WHO classification of tumours of the urinary system and male genital organs. A. Renal, penile, and testicular tumours. Eur Urol 2016;70(1):93–105.
18. Lopez-Beltran A, Carrasco JC, Cheng L, Scarpelli M, Kirkali Z, Montironi R. 2009 update on the classification of renal epithelial tumors in adults. Int J Urol 2009;16(5):432–443.
19. de Peralta-Venturina M, Moch H, Amin M, et al. Sarcomatoid differentiation in renal cell carcinoma: a study of 101 cases. Am J Surg Pathol 2001;25(3):275–284.
20. Leroy X, Zini L, Buob D, Ballereau C, Villers A, Aubert S. Renal cell carcinoma with rhabdoid features: an aggressive neoplasm with overexpression of p53. Arch Pathol Lab Med 2007;131(1):102–106.
21. Shinagare AB, Krajewski KM, Braschi-Amirfarzan M, Ramaiya NH. Advanced renal cell carcinoma: role of the radiologist in the era of precision medicine. Radiology 2017;284(2):333–351.
22. Schieda N, Thornhill RE, Al-Subhi M, et al. Diagnosis of sarcomatoid renal cell carcinoma with CT: evaluation by qualitative imaging features and texture analysis. AJR Am J Roentgenol 2015;204(5):1013–1023.
23. Young JR, Young JA, Margolis DJA, et al. Sarcomatoid renal cell carcinoma and collecting duct carcinoma: discrimination from common renal cell carcinoma subtypes and benign RCC mimics on multiphasic MDCT. Acad Radiol 2017;24(10):1226–1232.
24. Swartz MA, Karth J, Schneider DT, Rodriguez R, Beckwith JB, Perlman EJ. Renal medullary carcinoma: clinical, pathologic, immunohistochemical, and genetic analysis with pathogenetic implications. Urology 2002;60(6):1083–1089.
25. Iacovelli R, Modica D, Palazzo A, Trenta P, Piesco G, Cortesi E. Clinical outcome and prognostic factors in renal medullary carcinoma: a pooled analysis from 18 years of medical literature. Can Urol Assoc J 2015;9(3-4):E172–E177.
26. Dimashkieh H, Choe J, Mutema G. Renal medullary carcinoma: a report of 2 cases and review of the literature. Arch Pathol Lab Med 2003;127(3):e135–e138.
27. Amin MB, Smith SC, Agaimy A, et al. Collecting duct carcinoma versus renal medullary carcinoma: an appeal for nosologic and biological clarity. Am J Surg Pathol 2014;38(7):871–874.
28. Davis CJ Jr, Mostofi FK, Sesterhenn IA. Renal medullary carcinoma: the seventh sickle cell nephropathy. Am J Surg Pathol 1995;19(1):1–11.
29. Shah AY, Karam JA, Malouf GG, et al. Management and outcomes of patients with renal medullary carcinoma: a multicentre collaborative study. BJU Int 2017;120(6):782–792.
30. Prasad SR, Humphrey PA, Menias CO, et al. Neoplasms of the renal medulla: radiologic-pathologic correlation. RadioGraphics 2005;25(2):369–380.
31. Blitman NM, Berkenblit RG, Rozenblit AM, Levin TL. Renal medullary carcinoma: CT and MRI features. AJR Am J Roentgenol 2005;185(1):268–272.
32. Chao D, Zisman A, Pantuck AJ, et al. Collecting duct renal cell carcinoma: clinical study of a rare tumor. J Urol 2002;167(1):71–74.
33. Pickhardt PJ, Siegel CL, McLarney JK. Collecting duct carcinoma of the kidney: are imaging findings suggestive of the diagnosis? AJR Am J Roentgenol 2001;176(3):627–633.
34. Peyromaure M, Thiounn N, Scotté F, Vieillefond A, Debré B, Oudard S. Collecting duct carcinoma of the kidney: a clinicopathological study of 9 cases. J Urol 2003;170(4 Pt 1):1138–1140.
35. Srigley JR, Eble JN. Collecting duct carcinoma of kidney. Semin Diagn Pathol 1998;15(1):54–67.
36. Yoon SK, Rha SH. Collecting duct carcinoma. In: Guermazi A, ed. Imaging of kidney cancer. Medical radiology (diagnostic imaging). Berlin, Germany: Springer, 2006; 171–185.
37. Browne RF, Meehan CP, Colville J, Power R, Torreggiani WC. Transitional cell carcinoma of the upper urinary tract: spectrum of imaging findings. RadioGraphics 2005;25(6):1609–1627.
38. Miyazaki J, Nishiyama H. Epidemiology of urothelial carcinoma. Int J Urol 2017;24(10):730–734.
39. Prando A, Prando P, Prando D. Urothelial cancer of the renal pelvicaliceal system: unusual imaging manifestations. RadioGraphics 2010;30(6):1553–1566.
40. Humphrey PA, Moch H, Cubilla AL, Ulbright TM, Reuter VE. The 2016 WHO classification of tumours of the urinary system and male genital organs: part B—prostate and bladder tumours. Eur Urol 2016;70(1):106–119.
41. Vriesema JL, Aben KK, Witjes JA, Kiemeney LA, Schalken JA. Superficial and metachronous invasive bladder carcinomas are clonally related. Int J Cancer 2001;93(5):699–702.
42. Blacher EJ, Johnson DE, Abdul-Karim FW, Ayala AG. Squamous cell carcinoma of renal pelvis. Urology 1985;25(2):124–126.
43. Urban BA, Buckley J, Soyer P, Scherrer A, Fishman EK. CT appearance of transitional cell carcinoma of the renal pelvis. II. Advanced-stage disease. AJR Am J Roentgenol 1997;169(1):163–168.
44. Holmäng S, Lele SM, Johansson SL. Squamous cell carcinoma of the renal pelvis and ureter: incidence, symptoms, treatment and outcome. J Urol 2007;178(1):51–56.
45. Narumi Y, Sato T, Hori S, et al. Squamous cell carcinoma of the uroepithelium: CT evaluation. Radiology 1989;173(3):853–856.

46. Wimbish KJ, Sanders MM, Samuels BI, Francis IR. Squamous cell carcinoma of the renal pelvis: case report emphasizing sonographic and CT appearance. Urol Radiol 1983;5(4):267–269.
47. Richmond J, Sherman RS, Diamond HD, Craver LF. Renal lesions associated with malignant lymphomas. Am J Med 1962;32(2):184–207.
48. Hartman DS, David CJ Jr, Goldman SM, Friedman AC, Fritzsche P. Renal lymphoma: radiologic-pathologic correlation of 21 cases. Radiology 1982;144(4):759–766.
49. Miyake O, Namiki M, Sonoda T, Kitamura H. Secondary involvement of genitourinary organs in malignant lymphoma. Urol Int 1987;42(5):360–362.
50. Cohan RH, Dunnick NR, Leder RA, Baker ME. Computed tomography of renal lymphoma. J Comput Assist Tomogr 1990;14(6):933–938.
51. Reznek RH, Mootoosamy I, Webb JA, Richards MA. CT in renal and perirenal lymphoma: a further look. Clin Radiol 1990;42(4):233–238.
52. Chepuri NB, Strouse PJ, Yanik GA. CT of renal lymphoma in children. AJR Am J Roentgenol 2003;180(2):429–431.
53. American Cancer Society. Cancer Facts & Figures 2019. Atlanta, Ga: American Cancer Society, 2019.
54. Schwartz JB, Shamsuddin AM. The effects of leukemic infiltrates in various organs in chronic lymphocytic leukemia. Hum Pathol 1981;12(5):432–440.
55. Barcos M, Lane W, Gomez GA, et al. An autopsy study of 1206 acute and chronic leukemias (1958 to 1982). Cancer 1987;60(4):827–837.
56. Bach AG, Behrmann C, Holzhausen HJ, et al. Prevalence and patterns of renal involvement in imaging of malignant lymphoproliferative diseases. Acta Radiol 2012;53(3):343–348.
57. Araki T. Leukemic involvement of the kidney in children: CT features. J Comput Assist Tomogr 1982;6(4):781–784.
58. Hilmes MA, Dillman JR, Mody RJ, Strouse PJ. Pediatric renal leukemia: spectrum of CT imaging findings. Pediatr Radiol 2008;38(4):424–430.
59. International Myeloma Working Group. Criteria for the classification of monoclonal gammopathies, multiple myeloma and related disorders: a report of the International Myeloma Working Group. Br J Haematol 2003;121(5):749–757.
60. Knowling MA, Harwood AR, Bergsagel DE. Comparison of extramedullary plasmacytomas with solitary and multiple plasma cell tumors of bone. J Clin Oncol 1983;1(4):255–262.
61. Igel TC, Engen DE, Banks PM, Keeney GL. Renal plasmacytoma: Mayo Clinic experience and review of the literature. Urology 1991;37(4):385–389.
62. Abrams HL, Spiro R, Goldstein N. Metastases in carcinoma: analysis of 1000 autopsied cases. Cancer 1950;3(1):74–85.
63. Bracken RB, Chica G, Johnson DE, Luna M. Secondary renal neoplasms: an autopsy study. South Med J 1979;72(7):806–807.
64. Klinger ME. Secondary tumors of the genito-urinary tract. J Urol 1951;65(1):144–153.
65. Patel U, Ramachandran N, Halls J, Parthipun A, Slide C. Synchronous renal masses in patients with a nonrenal malignancy: incidence of metastasis to the kidney versus primary renal neoplasia and differentiating features on CT. AJR Am J Roentgenol 2011;197(4):W680–W686.
66. Zhou C, Urbauer DL, Fellman BM, et al. Metastases to the kidney: a comprehensive analysis of 151 patients from a tertiary referral centre. BJU Int 2016;117(5):775–782.
67. Sánchez-Ortiz RF, Madsen LT, Bermejo CE, et al. A renal mass in the setting of a nonrenal malignancy: when is a renal tumor biopsy appropriate? Cancer 2004;101(10):2195–2201.
68. Honda H, Coffman CE, Berbaum KS, Barloon TJ, Masuda K. CT analysis of metastatic neoplasms of the kidney: comparison with primary renal cell carcinoma. Acta Radiol 1992;33(1):39–44.
69. Choyke PL, White EM, Zeman RK, Jaffe MH, Clark LR. Renal metastases: clinicopathologic and radiologic correlation. Radiology 1987;162(2):359–363.
70. Bhatt GM, Bernardino ME, Graham SD Jr. CT diagnosis of renal metastases. J Comput Assist Tomogr 1983;7(6):1032–1034.
71. Craig WD, Wagner BJ, Travis MD. Pyelonephritis: radiologic-pathologic review. RadioGraphics 2008;28(1):255–277; quiz 327–328.
72. Foxman B. Epidemiology of urinary tract infections: incidence, morbidity, and economic costs. Am J Med 2002;113(suppl 1A):5S–13S.
73. Mitterberger M, Pinggera GM, Colleselli D, et al. Acute pyelonephritis: comparison of diagnosis with computed tomography and contrast-enhanced ultrasonography. BJU Int 2008;101(3):341–344.
74. Expert Panel on Urologic Imaging; Nikolaidis P, Dogra VS, et al. ACR appropriateness criteria: acute pyelonephritis. J Am Coll Radiol 2018;15(11S):S232–S239.
75. Majd M, Nussbaum Blask AR, Markle BM, et al. Acute pyelonephritis: comparison of diagnosis with ^{99m}Tc-DMSA SPECT, spiral CT, MR imaging, and power Doppler US in an experimental pig model. Radiology 2001;218(1):101–108.
76. Tsugaya M, Hirao N, Sakagami H, et al. Computerized tomography in acute pyelonephritis: the clinical correlations. J Urol 1990;144(3):611–613.
77. Dwivedi US, Goyal NK, Saxena V, et al. Xanthogranulomatous pyelonephritis: our experience with review of published reports. ANZ J Surg 2006;76(11):1007–1009.
78. Loffroy R, Guiu B, Watfa J, Michel F, Cercueil JP, Krausé D. Xanthogranulomatous pyelonephritis in adults: clinical and radiological findings in diffuse and focal forms. Clin Radiol 2007;62(9):884–890.
79. Kawashima A, Sandler CM, Ernst RD, Tamm EP, Goldman SM, Fishman EK. CT evaluation of renovascular disease. RadioGraphics 2000;20(5):1321–1340.
80. Dyer RB, Chen MY, Zagoria RJ. Classic signs in uroradiology. RadioGraphics 2004;24(Suppl 1):S247–S280.
81. Takahashi N, Kawashima A, Fletcher JG, Chari ST. Renal involvement in patients with autoimmune pancreatitis: CT and MR imaging findings. Radiology 2007;242(3):791–801.
82. Seo N, Kim JH, Byun JH, Lee SS, Kim HJ, Lee MG. Immunoglobulin G4-related kidney disease: a comprehensive pictorial review of the imaging spectrum, mimickers, and clinicopathological characteristics. Korean J Radiol 2015;16(5):1056–1067.
83. Saeki T, Kawano M, Mizushima I, et al. The clinical course of patients with IgG4-related kidney disease. Kidney Int 2013;84(4):826–833.